UNI-TR-9
UC-78

PHENOMENOLOGY AND MODELING OF PARTICULATE CORROSION PRODUCT BEHAVIOR IN HANFORD N REACTOR PRIMARY COOLANT

D. B. BECHTOLD

DECEMBER 31, 1983

UNC NUCLEAR INDUSTRIES

A UNC RESOURCES Company

P.O. Box 490
Richland, Washington 99352

Printed in the United States of America
Available from
National Technical Information Service
U.S. Department of Commerce
5285 Port Royal Road
Springfield, VA 22161
NTIS Price Codes
Printed Copy: A05
Microfiche Copy: A01

UNC NUCLEAR INDUSTRIES

Richland, Washington 99352

This report was prepared for use within UNC Nuclear Industries, Inc., in the course of work under supplemental agreement to the United States Department of Energy Contract DE-AC06-76RL01857. Any views or opinions expressed in the report are those of the author only. This report is subject to revision upon collection of additional data.

DOE-Richland, WA

UNI-TR--9

DE84 011833

PHENOMENOLOGY AND MODELING OF PARTICULATE CORROSION PRODUCT BEHAVIOR IN HANFORD N REACTOR PRIMARY COOLANT

by

D. B. Bechtold

PHENOMENOLOGY AND MODELING OF PARTICULATE CORROSION PRODUCT BEHAVIOR IN HANFORD N REACTOR PRIMARY COOLANT

TABLE OF CONTENTS

FIGURES

TABLES

APPENDIX

SUMMARY

Most of the radiation fields whose presence complicates maintenance work at Hanford N Reactor are the result of activated corrosion products (crud) being formed in the primary cooling loop. In response to this a program has been initiated to study and model the behavior of crud at N Reactor. One aspect of that behavior is the formation and fate of particulate crud in the coolant, and the present status of progress in this area is the subject of this report.

The instantaneous levels and approximate chemical composition of filterable corrosion products in the Hanford N Reactor Primary Loop are measurable by filtration of ca 40 Kg. of coolant onto 0.45 micron filters. Of 144 samples taken to date, the suspended crud level as determined by weight has ranged from 0.0005 ppm to 6.482 ppm with a median 0.050 ppm. There is considerable scatter but most determinations are within a factor of two of the median. The composition of the particulates approximates magnetite in appearance and chemical analysis.

The particle size distribution has been measured of particulates in coolant samples and has been found in 31 cases to be uniformly a log normal distribution with a count median ranging from 1.10 to 2.31 microns with a median of 1.81 microns, and the geometric standard deviation ranging from 1.60 to 2.34 with a median of 1.84. The particulate mass calculated from these distributions - based on the density of 5.18 gm/cc and octahedral shape - correlated with filter sample measurements with a slope of 1.0861 and an intercept of 0.014339, thus over-accounting for the true mass by 8%. The distribution of particulates during periods of high crud levels in the coolant was unobtainable, but was not expected to be very different in size distribution.

An auto-correcting inline turbidimeter was found to respond to linearly to suspended crud levels over a range 0.05 to at least 6.5 ppm by direct comparison with filter sample weights. This instrument was used to record continuous traces of particulate levels during reactor transients.

The overwhelming cause of "crud bursts" in the primary loop were found to be power decreases; upward power ramps do not produce detectable crud transients, nor do chemical transients, except during periods of otherwise high crud levels. The crud bursts of startups are shown to be the result of the previous shutdown and maintenance work.

The crud transients associated with a reactor power drop, several reactor shutdowns, and several reactor startups could be modeled consistently with each other using a simple stirred-tank, first order exchange model of particulate between makeup, coolant, letdown, and loosely adherent crud on pipe walls. Loosely adherent crud could be exchanged with tightly adherent crud through a sintering process and a loosening function which appears on power decreases or during the morphological relaxation of crud to hydrothermal conditions during a startup. The value of the deposition coefficient found was k_D = 0.00235 dm/min, of the erosion constant b = 0.00272 1/min, of the sintering constant c_T = 0.00370 1/min. The coefficient of crud loosening caused by a power drop rate dP/dt (Megawatt/min) averaged 0.476 microgram/dm^2/Megawatt. Morphological relaxation caused an exponential decay of crud loosening with an average time constant of 0.00977 1/min.

Over 3/10 of the average steady running particulate crud level could be accounted for by magnetically filterable particulate in the makeup feed.

A simulation model of particulate transport has been coded in FORTRAN based on the simple model to serve in conceptual design of a magnetic filter as part of another program. The model simulates particulate crud exchanges through a reactor startup, a run of selectable length with and without a magnetic filter of selectable flow and efficiency, and with a selectable letdown flow, and finally through a shutdown.

I. INTRODUCTION

Since 1977 there has been a small process development program at the Hanford N Reactor devoted to the study of activated corrosion product behavior in the primary loop. Here, as with every U.S. reactor vendor and numerous other organizations around the world, these corrosion products of the materials of construction are of great interest because their radioactivation and disposal in reactor cooling circuits cause adverse economic impact far out of proportion to their minute amounts (parts per billion in coolant). Indeed the principal reason for studying corrosion product (crud) transport at N Reactor, as elsewhere,[1,2,3] is to understand it sufficiently to formulate measures which mitigate the buildup of the resultant radiation fields.

The crud transport program at N Reactor began with the installation of a special primary coolant sampling facility[4,5,6] to provide a safe means to capture samples of the particulate and soluble crud for examination. The details of how the facility was actually operated, how it was shown to provide representative samples, and the full measure of the sampling program is the subject of another report to be issued soon.[7] As sampling progressed, it quickly became apparent that a supplemental reason for studying crud at N Reactor existed. N Reactor's rather unique design provided relatively large amounts of particulate crud. In fact, a scan of the general references 1, 2 and 3 shows that at least ten times as much circulated here--making for easier study--than at the typical power reactors, despite there being only 1/5 to 1/10 the magnitude of radiation fields at N Reactor at comparable primary loop components. The resolution of this seeming paradox must contain clues about crud behavior important to anyone seeking to lessen its adverse impact.

Of the several aspects of crud transport to be examined in order to build a useful understanding, the one which this report wll restrict itself to is the nature of and behavior of the particulate crud in the

coolant as opposed to soluble corrosion products or to the radionuclide content of crud. This is due mostly to an early emergence of understanding of particulate behavior and its precedent importance in treating other aspects, especially its relation to the actual source term of crud activation. Other reports dealing with radionuclide content, soluble crud, etc., will be issued when appropriate. Here, the convenient operational definition of particulate crud is that which can be filtered from the coolant with 0.45 micron filters, removed from piping walls and/or can be detected in coolant by turbidimetric means. There are five inter-related subtasks to be reported on here: Particulate Filter Samples, Particle Sizing Experiments, Continuous Turbidimetric Measurements, Analysis of Crud Transients, and Simulation Modeling of Particulate Crud. They will be dealt with in turn.

II. COOLANT FILTER SAMPLE EXPERIMENTS

To establish a baseline of information about the amounts, morphology and radionuclide content of filterable crud to be found in the N Reactor primary coolant, a program of daily samplings *via* the sampling facility was instituted. The complete description of the sampling facility in the detail necessary to document the adequacy of its performance is to be found in reference 7 and *loc. cit.* However, some details are provided here to demonstrate the representativeness of the samples; a point which is not trivial.

A. Filter Sample Method

The sampling Facility provides two 3/8" tubing sample streams from the primary loop, both of which may be accessed at temperature. However, both streams are cooled to approximately 60°C through separate U-tube heat exchangers after which either stream, by choice, may be directed through a sample line manifold and on to drain. Several Autoclave Engineers (R) valves are in each sample stream train and consequently their pressure drops limits each flow rate to approximately 1 gpm.

A sampling port tees off the sampling manifold at a point where there is still approximately 90 psi of back pressure (down from 1750 psi) and where opening this sample tap does not measurably perturb the continuous flow rate:

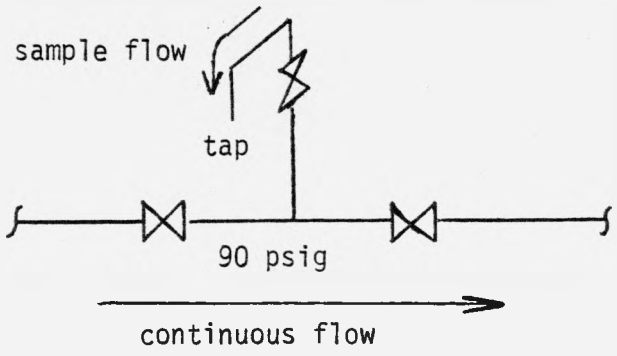

This is important, since perturbations of the sampling system flow can cause miniature crud bursts within the system, and thus compromise particulate sampling results. The turbidimeter, discussed later, has provided positive indication that the act of sampling does not induce detectable crud bursts within the sample lines.

During a sampling run, the technician establishes flow at the sample tap to flush it out and to catch a 500 cc grab sample for particle size experiments. The flow in the sampling manifold runs continuously. He then attaches two 47 mm membrane filter holders in series each loaded with one of a Millipore, Inc. matched-weight 0.45 micron filter pair (one "sample" and one "blank") and filters up to 40 kg. of coolant, catching 500 cc. of the filtrate for subsequent analysis. The filtrate is weighed on a scale. The filtration takes approximately 20 minutes, during which time the technician is performing the particle size experiments to be discussed later.

Back in the lab, the technician dries the filter pairs in a vacuum oven and weighs them individually on an analytical balance. Their weight difference, typically a few milligrams, represents the filterable crud mass per the weight of filtrate. The filters are matched to within 0.1 milligram, and their use saves a great deal of preparation time. The filters are subsequently used in a variety of determinations, radiochemical and chemical, of their content.

B. Filter Sample Results

To date 144 filtered samples of coolant corrosion products have been acquired. Most of the samples represent equilibrium reactor operations, but a few were taken during crud transients.

The filter samples invariably captured very finely divided, black deposits ranging from 0.0005 ppm to 6.4 ppm, with a median of 0.0505 ppm. Analysis of the filter samples via atomic absorption spectroscopy has had disappointing reproducibility, but results suggest mostly magnetite with nickel, manganese and chromium in the low parts per thousand. Cobalt analyses by spectroscopy are not yet trustworthy. Magnetite is the expected corrosion product, given that the reactor operates with 130,000 ft^2 of carbon steel surface, approximately 18 ppm ammonia and as a consequence approximately 2 ppm dissolved hydrogen, 8 ppm dissolved nitrogen, and undetectable dissolved oxygen at the ppb level.

Among the other calculations made using the filtered crud mass results, two very important ones to be discussed next are verification of the particle size data and calibration of the turbidimeter.

III. PARTICLE SIZING EXPERIMENTS

To complement the filter sample data a simultaneous series of particle sizing experiments was carried out during the period late 1978 to late 1981. Within this time, data collected from 1979 through February, 1980, the particle sizing instrument worked reliably enough to give trustworthy data. Of necessity these experiments had to be carried out in the radiation zone at the sampling facility, a zone of 110-120°F and high humidity ambient conditions, in order to gather results before sample agglomeration occurred.

A. Particle Sizing Experimental Method

After the technician had run the sample tap described in Section II.A. for a few minutes, he would capture a 500 cc poly bottle of coolant and set it aside to cool and degas while setting up the filter holders. After no more than 5 minutes elapsed time he would draw the sample through the sensing head of the particle sizing instrument to perform the measurement, in the following arrangement:

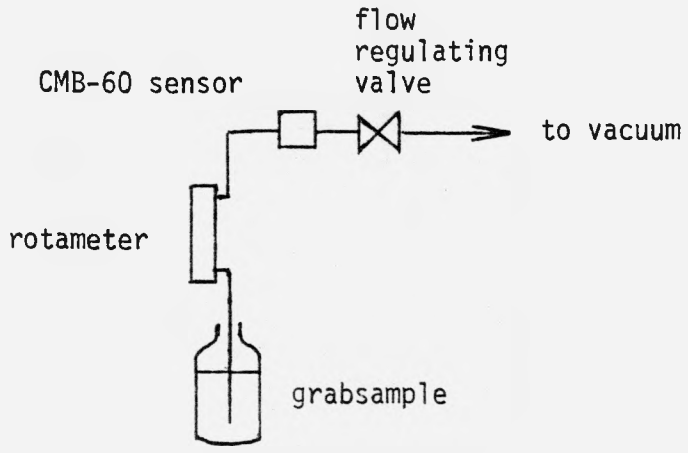

The particle sizer was a HIAC model PC-320 with nine sizing channels, employing the model CMB-60 sensing head (1-60 micron range) which required 8 $\pm$ 1/2 ml/min flow rate to work properly. A Dwyer rotameter (0-10 ml/min) was used in conjunction with the valve to adjust flow. Vacuum was provided by a small diaphragm

vacuum pump working through a vacuum flask. Before each run the technican would clean out the sensing head, and during the run he would watch to be sure that no bubbles would evolve in the flowmeter to compromise the particle count. Each count run would be for 99 seconds, and the instrument would be in the integrated mode, i.e., each channel representing the accumulated counts of particles ranging in size between the channel setting and 60 microns. The channels were set to provide a reasonably even span between ln(1) = 0 and ln(10) = 2.3 for reasons to be made clear. The certified factory calibration data against spheres was relied upon for the instrument calibration.

B. Particle Sizing Analysis Method

The principle of instrument operation used to size the individual crud particles was light blockage. As each particle passes through the active zone, tumbling as it goes, it casts a shadow on a photodiode on one side of the zone due to there being a light source on the other. The maximum shadow it casts causes a current pulse minimum in the output of the photodiode which is pulse-height analyzed and put into the appropriate size channel.

To equate a particle diameter with a given sized shadow and therefore a given channel setting, the instrument is calibrated against spherical particles. Its channel settings represent the diameter of the sphere that casts a shadow equal to the (possibly irregular) particle of interest.

Preliminary results indicated that the typical size distribution approximated a log normal distribution, and it was decided that all subsequent experiments would be examined in terms of such a distribution. Therefore each set of data (nine channel settings and accumulated counts) was least squares fit to the following expression:

$$n_i = \frac{N}{\sigma\sqrt{2\pi}} \int_{\ln(d_i)}^{\ln(60)} \exp\left\{ - \frac{(x-\mu)^2}{2\sigma^2} \right\} dx \qquad (1)$$

$$= \frac{N'}{2} \pm \operatorname{erf}\left\{ \left| \frac{\ln d_i - \mu}{\sigma\sqrt{2}} \right| \right\} + \operatorname{erf}\left\{ \left| \frac{\ln 60 - \mu}{\sigma\sqrt{2}} \right| \right\}, \quad \mu \mp d_i \geq 0$$

$$d_i, \mu \leq 60$$

$$i = 1 \longrightarrow 9$$

where i = channel number,

d_i = channel setting equivalent spherical diameter,

μ = natural log of count median or geometric mean,

σ = natural log of geometric standard deviation, and

N = total counts in the sample.

A computer program was used[8] to do the least squares fitting, converting the channel setting to equivalent spherical diameter after the calibration curve of the instrument, and using μ, σ, and N as adjustable parameters. The output of the fitting program, both printed and plotted, was used to judge the prior assumption of a log normal distribution in each experiment, which the fitting results in all cases justified.

It was desired to obtain the calculated mass of the particle in a sample for comparison with the filter sample results, and also to determine the surface area of the particulate crud. After having demonstrated a log normal particle distribution, it becomes a matter of relating the equivalent spherical diameter to the actual area and volume of the magnetite crud particles. This is done by first assuming that each particle in a sample was a perfect octahedron, the expected crystal morphology of magnetite. The maximum projected area of a octahedron, or shadow cast, is that projection parallel to its four-fold symmetric axis--an area equal to z^2, where z is the length of a side. The projected area of a sphere, against which the channel settings of the instrument were calibrated, is π "d"$^2/4$, where "d" is the equivalent spherical

diameter which the instrument associates with the individual particle. With our assumption of octahedral particle shape, this means:

$$"d" = 2z/\sqrt{\pi} \tag{2}$$

We are now in a position to determine the octahedral area and volume of a particle in terms of its associated "d" value. The volume of an octahedron v is $\sqrt{2}\, z^3/3$ and its surface area s is $2\sqrt{3}\, z^2$; we merely substitute equation (2) for z in these expressions to obtain:

$$v = \frac{\pi^{3/2}}{12\sqrt{2}} "d"^3 \tag{3}$$

and,

$$s = \frac{\pi\sqrt{3}}{2} "d"^2 \tag{4}$$

To continue towards the specific mass and specific area of the collection of particles in a counting sample, we note that the total volume of the particles we measure is the integral of equation (3) over the log normal distribution of the particles characterized by N, μ, σ. The same is true for the total surface area; integrate equation (4) over the same distribution. Hence, the specific mass of particulates of density 5.18 gm/cc (the x-ray theoretical density of magnetite) in a sample stream analyzed at the rate of 8 cc/min for 99 seconds and whose fluid density was 0.997 gm/cc works out to

$$\text{Sp. mass (ppm)} = \frac{60 \times 10^{-6} \times 5.18 \times \pi^{3/2} \times N}{0.997 \times 99 \times 8 \times 12 \times \sqrt{2} \times \sqrt{2\pi} \times \sigma} \int_{\ln(A)}^{\ln(B)} \exp\left\{3y - \frac{(y-\mu)^2}{2\sigma^2}\right\} dy \tag{5}$$

Where y is the natural log of "d" measured in microns, and A and B approximate zero and infinity accurately enough. For the present, A = 0.001 and B = 1000 are sufficient for numerical integration. Likewise, the specific area works out to:

$$\text{Sp. Area } (cm^2/gm) = \frac{60 \times 10^{-8} \times \pi \times \sqrt{3} \times N}{0.997 \times 8 \times 99 \times 2 \times \sqrt{2\pi} \times \sigma} \int_{\ln(A)}^{\ln(B)} \exp\left\{2y - \frac{(x-\mu)^2}{2\sigma^2}\right\} dy \quad (6)$$

and we have the required expressions.

Evaluation of the specific mass and specific area for each experiment was left to the same computer program that determined the best fit of the log normal distribution to each sample.

To summarize the analysis of the particle sizing data, the nine channels of count data for each sample were used to fit a log normal distribution of equation (1) by weighted least squares (weights derived from the Poisson statistics of each count and the uncertainties in the instrumental calibration) to determine the parameters μ, σ, and N for the sample. The output of the fit verifies the assumption of a log normal distribution. Next, the computer program calculates the specific mass and specific area of the particulates in the sample based on the fitted parameters via Equations (5) and (6). The calculated specific mass should be directly comparable to the ppm derived from the filter sample experiments performed at the same time.

C. Particle Sizing Results

Approximately 50 particle sizing runs were made as part of the coolant sampling program. Figure 1 shows a typical result of fitting a log normal distribution to a nine-channel cumulative sizing experiment. Note that the fitted distribution corresponds to a geometric mean = e^{μ} = 2.2 microns, and a geometric standard deviation = e^{σ} = 1.68. The range of the sensing head used is 1-60 microns and as the Figure shows there are some particles to be expected below one micron in equivalent spherical projection diameter. The act of using this fitted distribution to calculate a specific mass is an extrapolation below 1 micron

FIGURE 1

TYPICAL CUMULATIVE PARTICLE SIZING RESULT

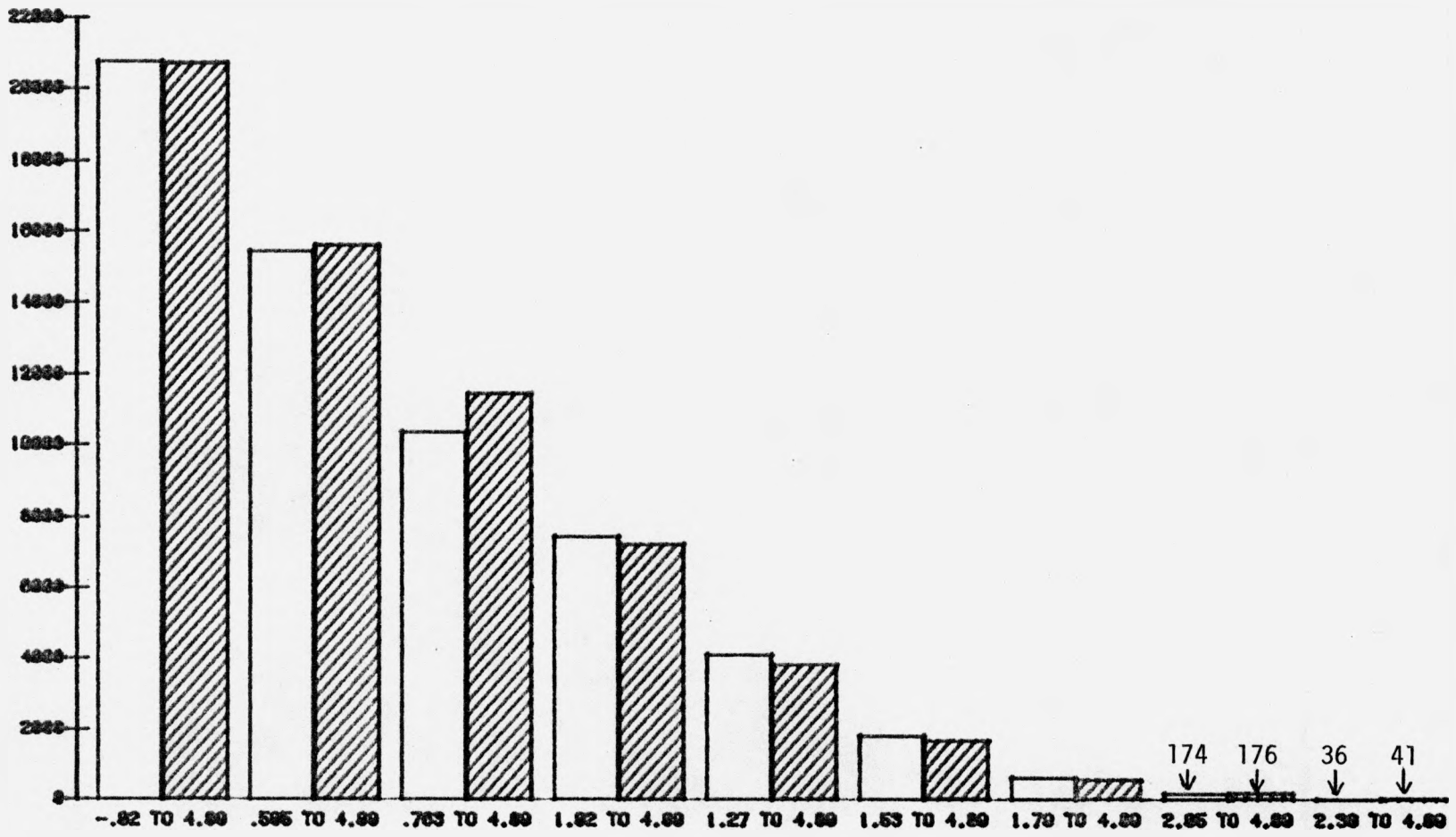

ln(microns) Size Interval

CUMULATIVE COUNT DATA (to 60 microns)

LOG NORMAL FIT (μ = .788, σ = .521, N = 22130)

and above 60 microns. This is not of much consequence, however, since virtually all the mass represented by this distribution seems to be accounted for.

Figure 2 shows a direct comparison of the specific mass of particulates in coolant as calculated from the particle sizing experiment with the filterable specific mass discussed in Section II. The Figure demonstrates two important facts:

a) the method works for low levels of crud--there is a direct linear correlation (shown in the key) with a slope of 1.08 and an intercept of 0.014 ppm. The smallness of the intercept implies that carryover of particulates in the particle sizing apparatus is not a problem, i.e., a new sample is not appreciably contaminated by previous samples. All of the assumptions about particle shape and density, and the extrapolations of the fitted distributions to unmeasured regions result in a mere 8% error in calculated specific mass, as shown by the slope. The linear response at low levels of crud is further evidence that the method is responding cleanly to actual crud levels in the grab samples, and that carryover is negligible.

b) the instrument fails at high crud levels--the data points associated with crud levels greater than 150 ppb are too scattered to be useful. The HIAC instrument has an indicating light to show when its counting capacity is being overloaded by the simultaneous light blockage of two or more particles. However, the points plotted as "high crud levels" were thought to be successful counts. There is a clear demonstration here of counting overload which limits the usefulness of the particle sizing data to crud levels associated with equilibrium reactor operation.

FIGURE 2

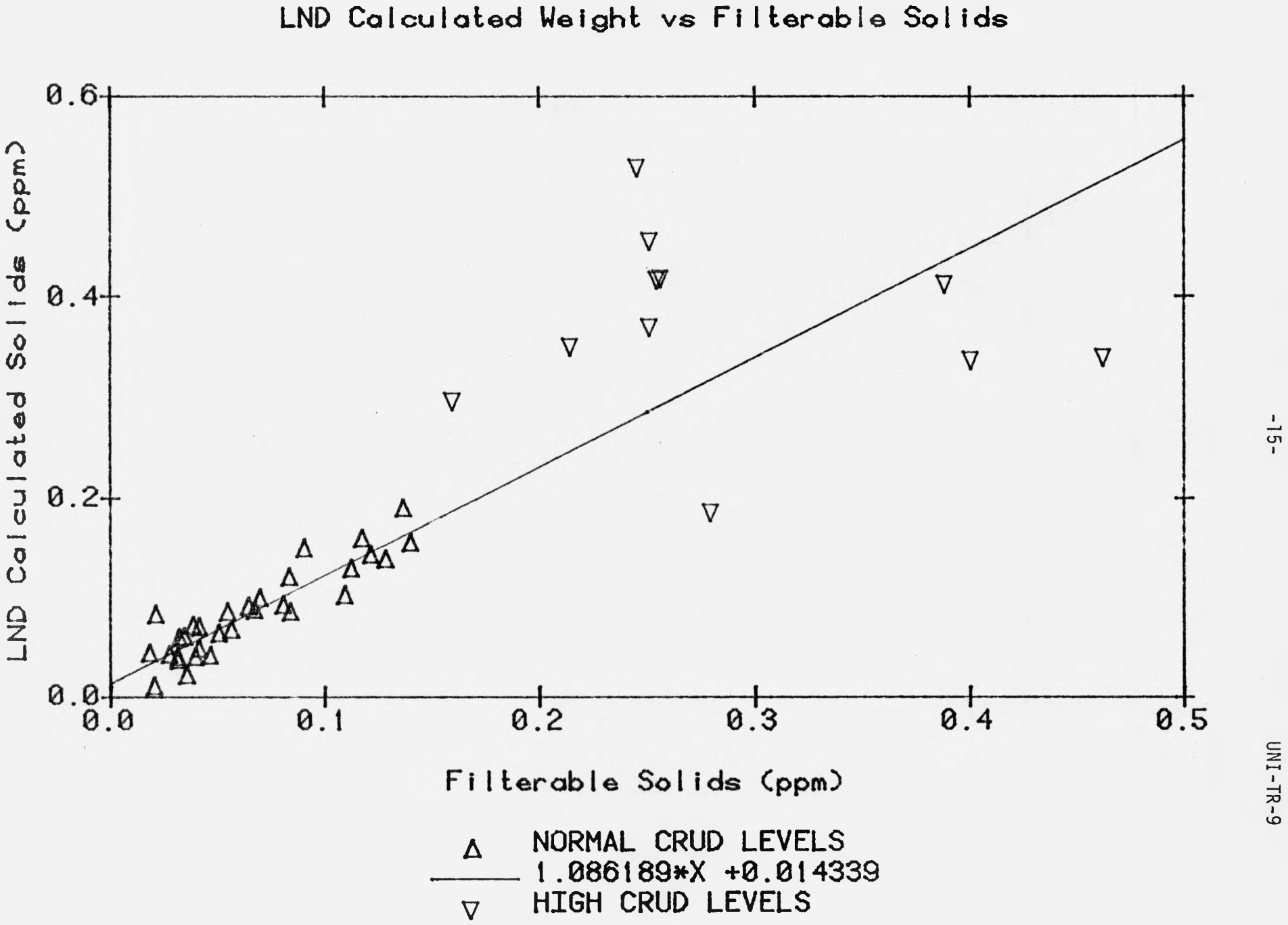
LND Calculated Weight vs Filterable Solids
LND Calculated Solids (ppm)
0.6
0.4
0.2
0.0
0.0
0.1
0.2
0.3
0.4
0.5
Filterable Solids (ppm)
NORMAL CRUD LEVELS
1.086189*X +0.014339
HIGH CRUD LEVELS

Figure 3 demonstrates one more important point about the particulates in primary coolant during steady operation: the shape of the distribution changes very little with crud level, only the total number of particles changes appreciably. Of the 31 low-level particle sizing experiments which were valid, the geometric mean ranged from 1.10 to 2.31 microns, with an average of 1.81 microns and a relative standard deviation of 20%. The geometric standard deviation in turn ranged from 1.60 to 2.34, averaged 1.84 with relative standard deviation of 22%. These numbers are of no formal statistical significance, but they convey the regularity of the size distribution over the operating conditions it was measured. Figure 3 reflects this in that if the shape (e^{μ} and e^{σ}) of the distribution does not change, then the area and mass of the particulates are in constant proportion. For clarification it should be pointed out that the ordinates of Figure 3 are in units of cm^2 per gram of coolant.

It was hoped that a large variation in distribution shape would be detected so that specific area and specific mass would not be so much in lock step. Then, filterable radionuclide activities could be plotted against specific area and specific mass to make a determination whether nuclides were uniformly absorbed throughout the particles or merely adsorbed on their surfaces. The uniformity of distribution shape obviates any comparison of this kind.

The uniformity of particulate distribution is not surprising when one compares these findings with two rather important references.[9,10] Reference 9 is a comparable report which predates much of this work, at the Winfrith SGHWR. This reactor is a smaller pressure tube BWR, but it has a similar circulating surface-to-volume ratio to N Reactor's pressurized primary loop. At Winfrith, the reported equilibrium operation crud levels were fairly similar to the present findings. In addition, the authors' rather more extensive particle sizing work showed log normal distributions only slightly larger in geometric mean diameter. These distributions were shown to remain approximately the same shape during crud transients as well.

FIGURE 3

LND SPECIFIC AREA VS FILTERABLE SOLIDS

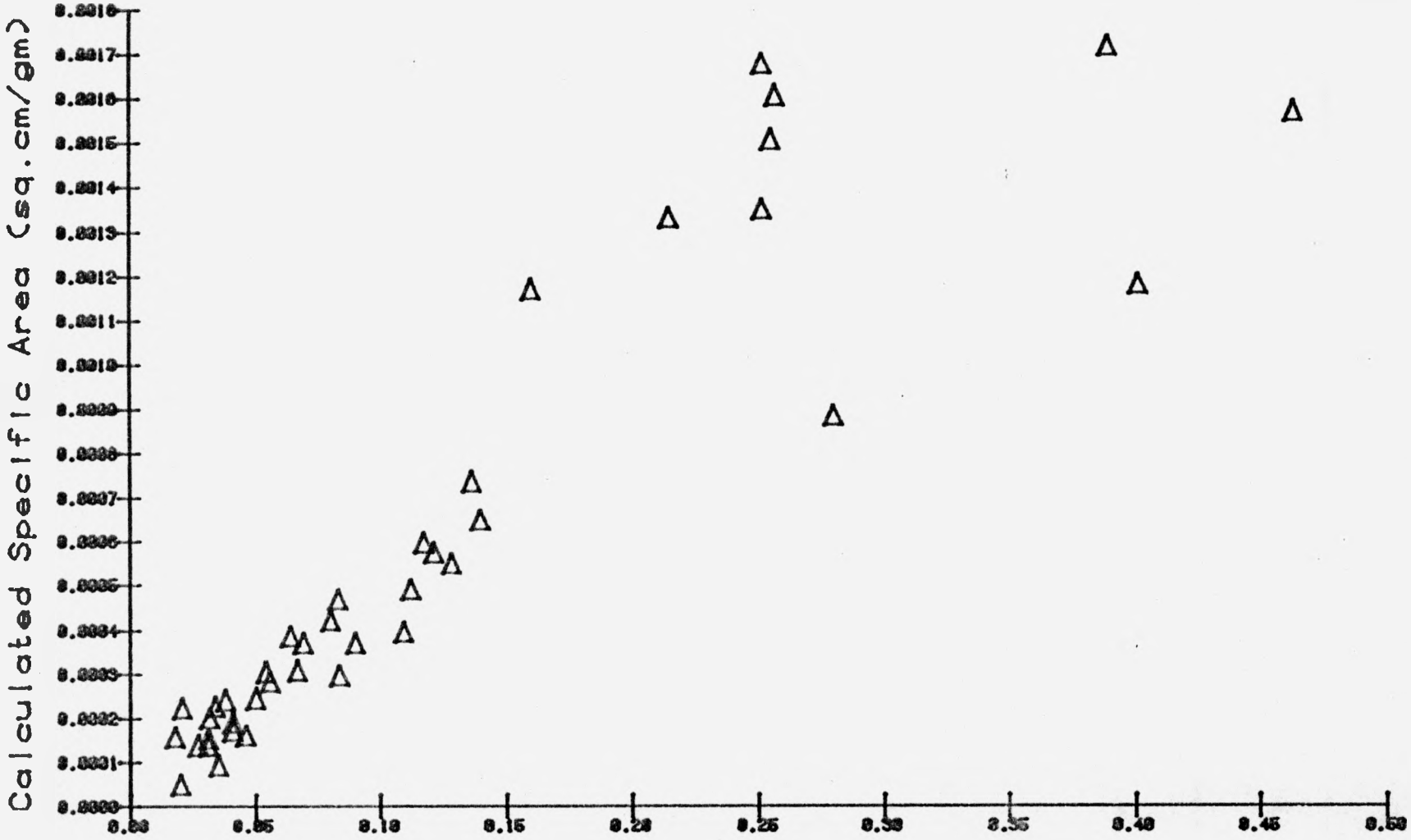

Reference 10 calculates likely agglomeration and breakup rates of particles in primary loops of reactors, based on particle strengths and flow conditions. The conclusion is that agglomeration is not a signficant process in modifying particle size distributions or in affecting particle deposition rates. The high shear stresses in primary pumps can be expected to quickly reduce large, vulnerable particles to an equilibrium size distribution if they did form, perhaps during the shedding of piping crud during a power ramp.

The comparison of the present work with the literature leads to the general notion of a rather stable, unchanging particle size distribution in primary circuits, despite large changes in total crud levels. Apparent overall particulate deposition rates would then be unaffected by nonexistent changes in size distribution, and hence the crud may be viewed as a material having an overall uniform behavior towards deposition and erosion.

IV. CONTINUOUS TURBIDIMETRIC ANALYSIS

Daily samples of primary coolant are a poor way to characterize the behavior of crud transients (crud bursts) in reactor primary loops. Crud transients hold the information necessary to elucidate deposition and resuspension kinetics and mechanisms, therefore a means for continuous monitoring and recording of crud levels in the N Reactor primary loop was sought early in the program. An allusion to "Aphimetre" contained in Reference 11 promised a linear response to crud levels in water. Based on this a Gam Rad Model 370-A (turbidimetric) Fluid Analyzer with optional cooling coil was purchased and installed on the sampling facility. Its output was connected up to the L&N strip chart recorder and the results, as explained below, were very satisfactory.

A. Continuous Crud Monitoring Method

The Gam Rad turbidimeter sensor was plumbed into the sampling facility low temperature sampling line in the following schematic arrangement to provide an adequate flow of sufficient back pressure to ensure that no evolution of dissolved gases occurred in the sensor.

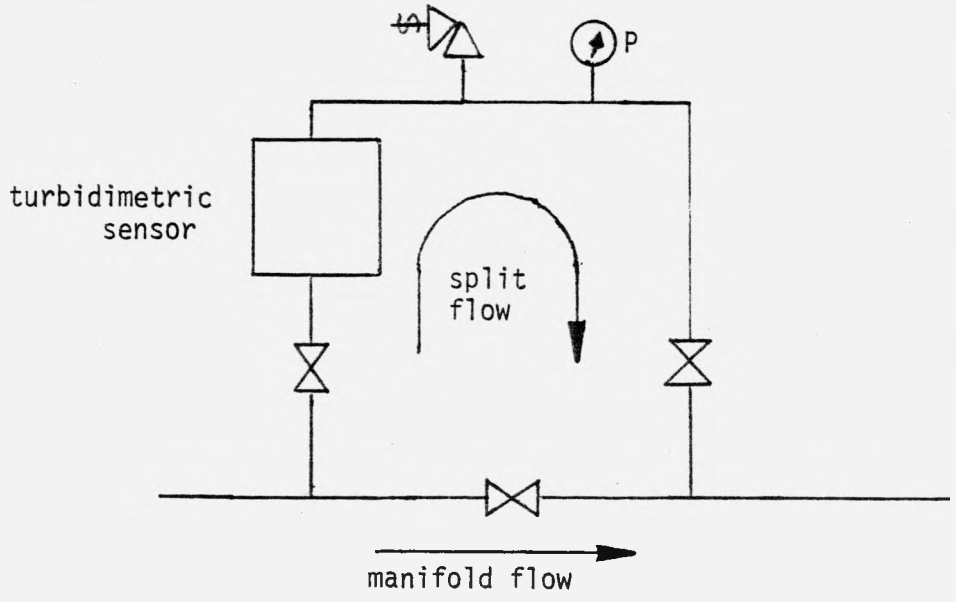

The turbidimeter has a dual light path with compensating circuits to allow it to automatically adjust for changes in coolant color or buildup of crud on the windows. The meter had a x1 and x10 scale. The zeros and slopes of these scales were matched as closely as possible and the auxiliary output was sent to the strip chart recorder set to advance the paper at 1"/hr. The recorder has a 0-100 scale, which was adjusted to match the turbidimeter output.

The whole system ran whenever the sampling facility was operating in order to catch crud transients as completely as possible. The reading of the meter was read simultaneously with every filter sample run in order to build up a calibration data set, and every week the previous week's chart was removed for examination of reactor transients.

B. Turbidimeter Operating Results

The analyzer turned out to be very stable and easy to maintain under the adverse conditions of its operation. Equilibrium operation of the reactor produced an indication of 5-10% of full scale on the x1 setting, and very strong responses were made to crud transients, including those caused by starting up the sampling facility itself. A very useful result of the analyzer was its lack of indication whenever a filter sample run was made. This verified that filter samples were sampling the primary coolant as intended and not a load of perturbed crud from the sampling system tubing. In Reference 7 is detailed how the analyzer's response to sampling system switching was used to analyze the sampling system performance.

The very important matter of the analyzer's response to crud levels was resolved by comparing the meter readings taken during sampling runs with the filter sample results. Figures 4 and 5, both plots

FIGURE 4

FILTERABLE SOLIDS VS TURBIDITY

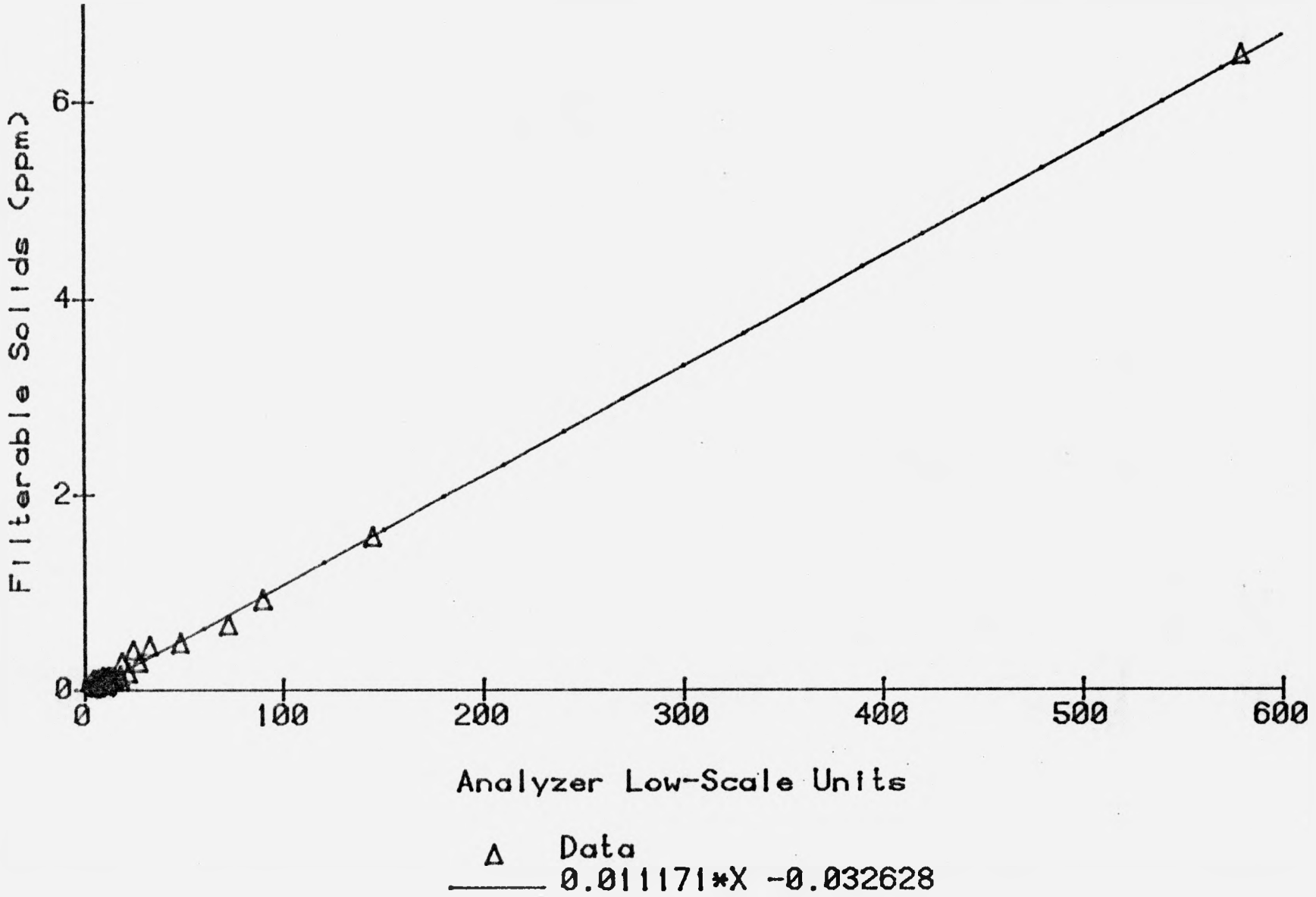

FIGURE 5

FILTERABLE SOLIDS VS TURBIDITY

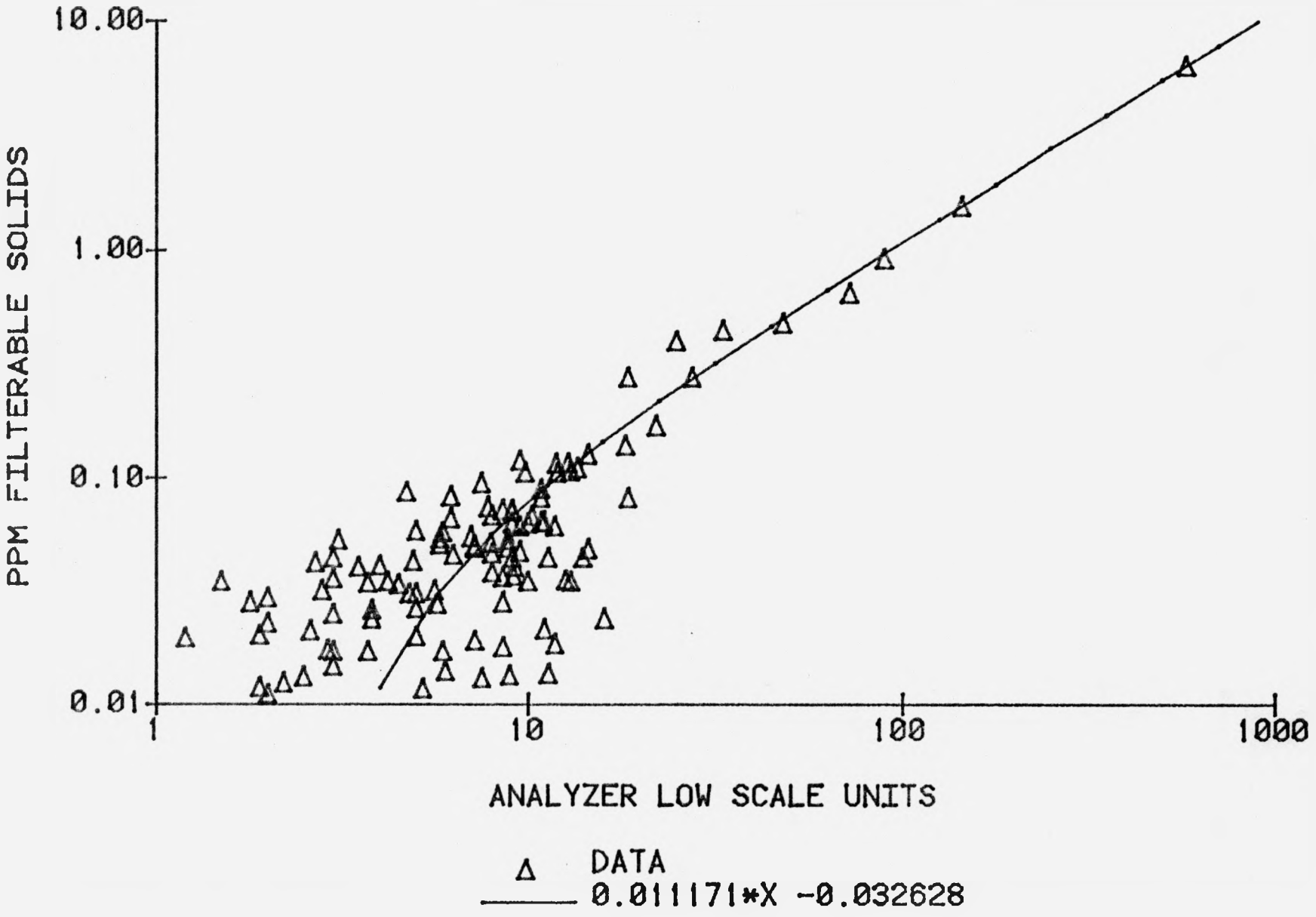

of the same data, indicate that the response of the analyzer to crud levels is linear at least to 6.5 ppm. Analyzer readings above 100 are the conversion of high (x10) scale readings to consistent units. The higher data points which define the linearity are the fortunate result of filter sample/meter readings taken during crud transients. Figure 5, on the low end, shows the kind of statistical reproducibility inherent in the filter sample method. The analyzer response was generally steady at low values, but there were some indications of long term drift in the instrumental baseline. The slope of the linear fit, presently 0.01117, moved about somewhat as the data set was being built up but never varied more than 15%. With this assurance of a linear response and an absolute calibration, it became possible to use the crud level traces provided by the instrument to determine particulate crud deposition/resuspension behavior in the reactor primary loop.

V. CRUD LEVEL TRANSIENT ANALYSIS

The observation of systems at steady state yields little information about the kinetic workings within the system. To determine kinetics, changes to provoke responses are necessary. So it is with crud transport in reactor primary loops. The steady running, "equilibrium" operation of the reactor produces an equally steady level of particulate primary loop crud. This level can be the result of any combination of crud in the makeup stream, crud flaking off of pipe walls, crud precipitating out of solution, etc. When known perturbations occur, the resultant burst of crud and its relaxation back to steady state might possibly be interpreted in ways useful to understanding crud transport of radionuclides.

A. Crud Transient Data Collection/Reduction Method

Section IV. explains the setup used to continuously record crud levels in the primary loop. On a weekly basis the strip chart was examined for interesting crud level transients. Besides the crud level, the strip chart contained traces of coolant pH, conductivity, sample line temperature, primary loop hot leg temperature, cold leg temperature, and automatic hourly markings of the time of day. When an interesting transient occurred, operations information from the Console Log and other sources was gathered independently to document the power and/or chemistry conditions which caused it. The trace was subsequently digitized on a Hewlett Packard digitizer, and the resulting time series of x (time), y (response) data pairs were read into computer files for further analysis. The units of time, scale divisions, and instrument calibration were noted so that conversion of the digitized data to absolute units could be made. In the case of crud levels, the calibration curve of Figure 4 was used.

B. Crud Transient General Features

Reference 7 recounts the analysis showing that the response of the fluid analyzer to primary loop crud transients was not appreciably affected by the sampling system itself. With that in mind the examination of the crud transients observed produced some interesting general features.

The first result is that the changes in water chemistry generally did not produce any crud transients. Even the most massive documented pH drop (ammonia is the pH additive) ever recorded failed to produce anything other than a possible slow shift in baseline after 18 hours. Out of more than five chemical transients examined, only two exceptions were found. They were the result of massive, sudden increases in ammonia injection occurring in the middle of reactor startup crud bursts. Compared to the crud burst already in progress, the crud transient produced was in both cases small and of short duration (they will be pointed out later). These exceptions are in themselves fascinating and probably have much to say about the fundamental coupling between magnetite solubility and crud transport. However, their analysis is postponed to a future report, and they are indeed exceptions; nothing like them has been observed during equilibrium operation despite several opportunities.

The second general feature is that nearly all crud transients are very slow (6-1000 minutes) compared to the circulation time (0.74 minutes) in the primary loop, indicating that the loop behaves as a stirred tank towards the buildup and loss processes of suspended crud.

Thirdly, the significant crud bursts that were encountered all had something to do with power or changes in pump speed. Furthermore, they could be reproducibly categorized into 4 main causative groups: Power Drop, Normal Shutdowns, Scrams, and Startups. These will be described in turn.

1. Power Drop Crud Burst

Unfortunately, only one crud burst documented to be due to this kind of event has been recorded to date. The digitized version of the crud trace is shown in Figure 6, along with the reactor power. It was fortuitously the ideal small perturbation; Operations decided that the reactor would have to be shut down and so the standard power ramp from 3805 megawatts was executed. However, before 10% of the power was cut in 5 minutes the perceived problem was remedied and power was held. After a delay the power was slowly brought back up to former levels.

The crud level in the primary loop took a smooth but strong rise correlated to the minute with the start of the "shutdown" (with suitable allowances for sample line holdup-time see Reference 7) and continued to execute what appeared closely to be a two-exponential-decay, i.e., the kind of curve described by $Ae^{+bt} + Be^{-bt} + C$.

It should be noted that the crud level did not discontinuously jump to some level, rather it quickly-but-smoothly began an upward ramp. Clearly a large amount of crud was not instantly released into the primary loop by the first power drop, but some process was indeed initiated to be a decaying source for suspended crud. In addition the bumps appearing in the data do not correlate with the subsequent power rises on close examination in any logical, cause and effect manner; i.e., the power rises do not seem to add anything to the ongoing crud burst, as might have been expected.

2. Normal Shutdown Crud Bursts

The standard normal shut down consists of a linear power ramp down from 3800-4000 MW to a few hundred MW, followed by some small ramps to complete shutdown interspersed with short holds. This process takes about an hour, and represents the extension of the power drop described in the last section.

CRUDBURST OF 3/26/80

FIGURE 6

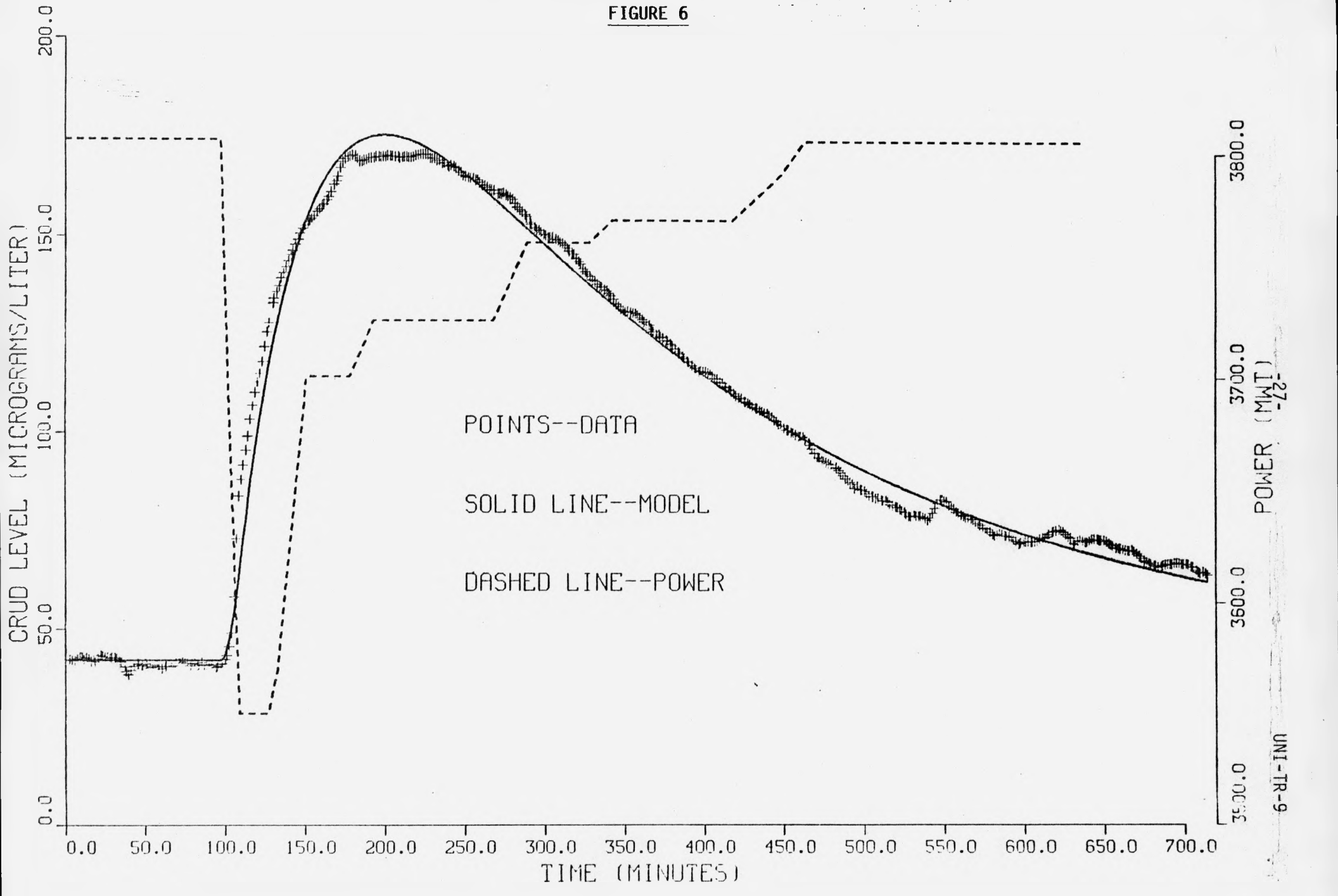

Three of many very similar crud transients caused by normal shutdowns and correlated very closely to the start of the power ramp are shown in Figures 7, 8 and 9. Note the smooth transition from the steady state level to the nearly linear rate-of-rise executed by the crud trace. This can be viewed as an extension of the process creating the source term for the power drop crud burst, but for a much longer continuous time.

What is not shown in Figures 7, 8 and 9 is the trace after pump trip-off. Correlated with this event is a break in the crud level trace to lower, random wanderings. The sampling system by its nature[7] depends on full primary pressure and full primary loop flow to adequately sample the loop contents. Pump trip-off removes this necesary condition, unfortunately, and invalidates any serious intepretation of sampling system data thereafter. In any case, the moment of pump trip-off is clearly evident in shutdown traces and the data displayed in Figures 7, 8 and 9 are free of any such compromise.

3. Scram Crud Bursts

N Reactor scrams fairly often and the crud bursts accompanying scrams are all very similar. Unfortunately a scram is immediately followed by a pump trip and depressurization, so as not to cool the primary loop too rapidly, and meaning that the crud traces are unreliable. What happens is that the crud trace suddenly undertakes a very rapid rise taxing the ability of the multipoint recorder to follow it. The rise goes to nearly the top of the low scale before the effects of the pump trip cause it to drop off and wander.

4. Startups

An N Reactor Startup is normally as follows: At system pressure and half-speed on the primary pumps, the reactor is brought up to something less than 650 Megawatts. At this point

FIGURE 7

SHUTDOWN CRUD BURST 2/8/80

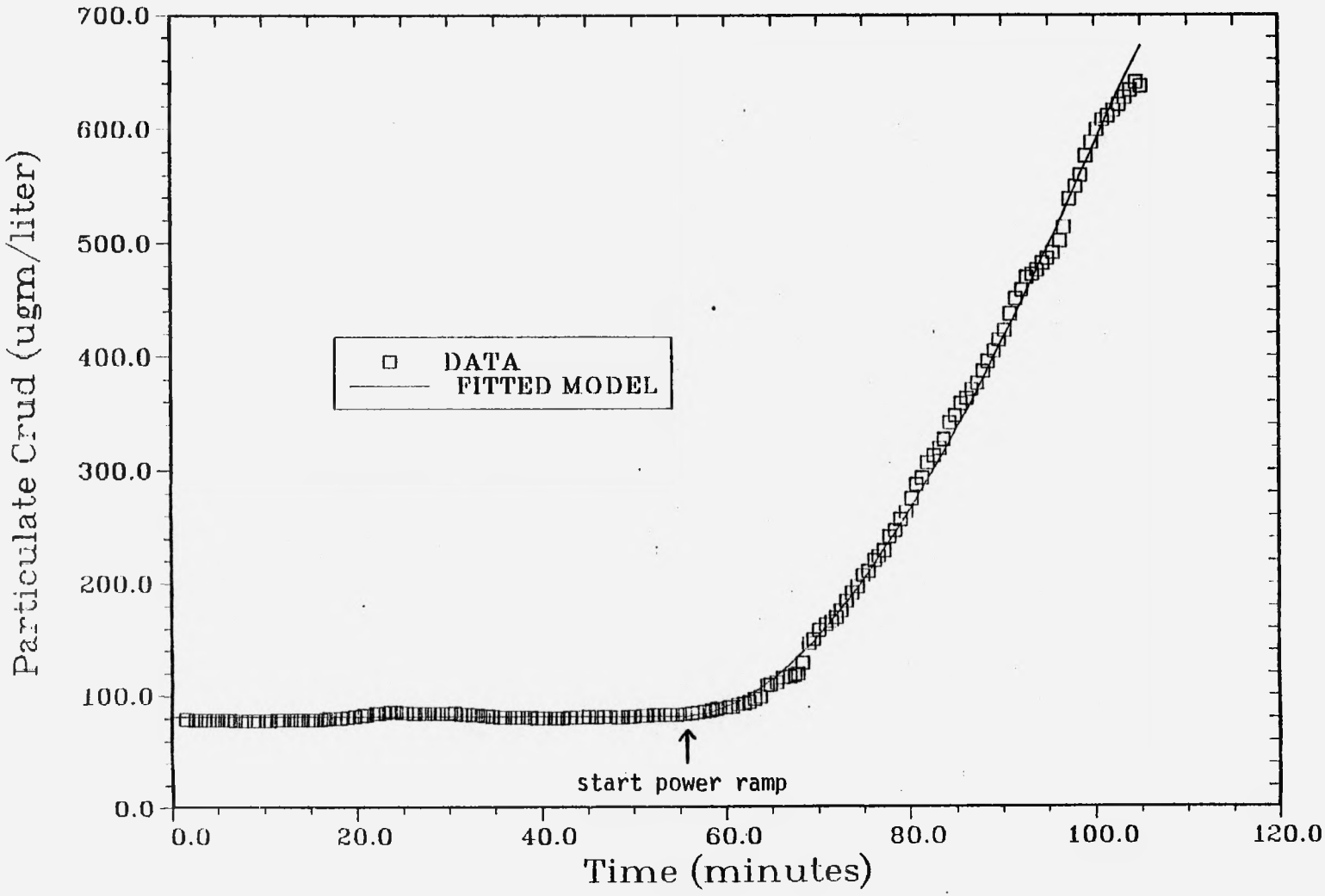

FIGURE 8

SHUTDOWN CRUD BURST 3/1/80

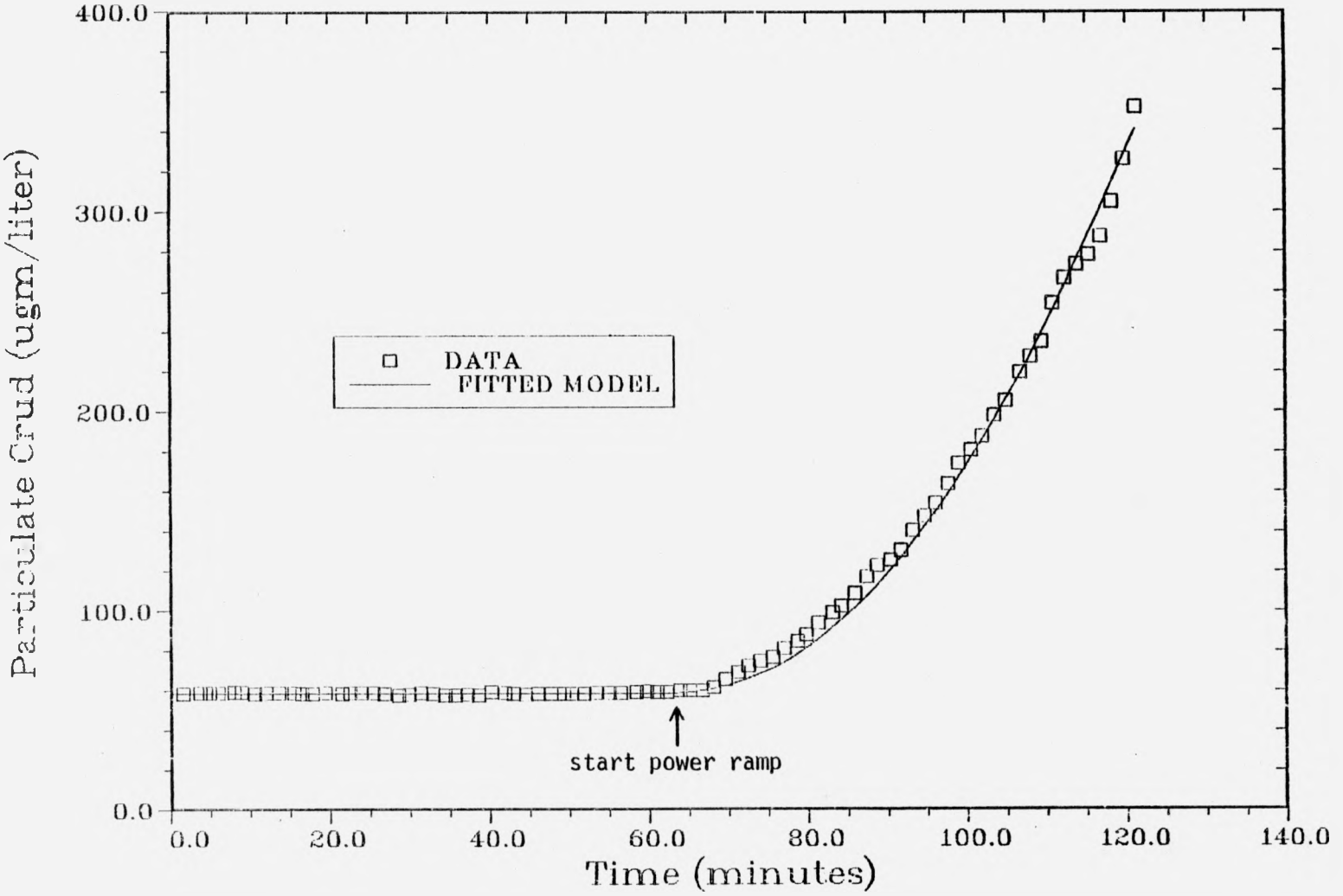

FIGURE 9

SHUTDOWN CRUD BURST 5/13/80

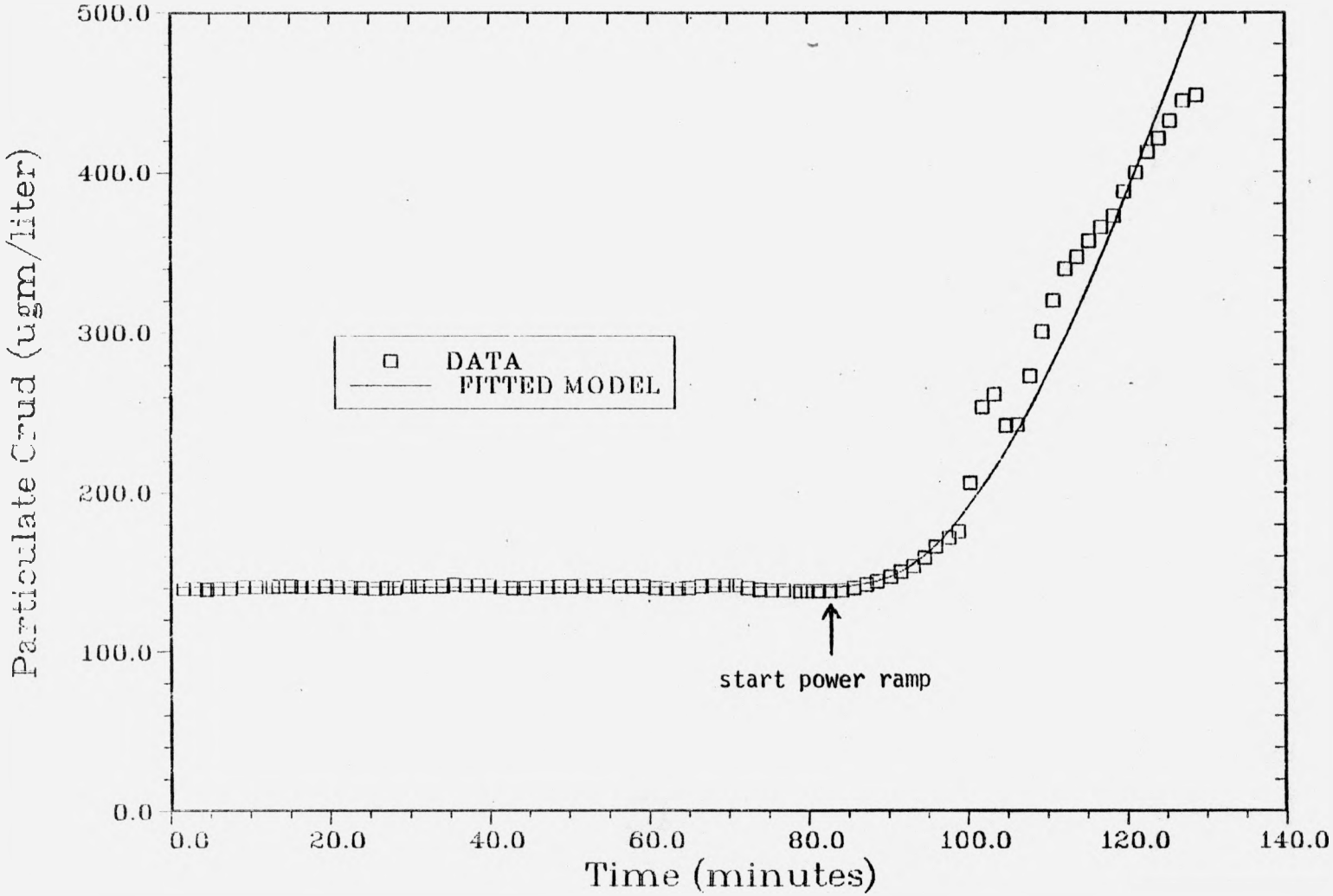

a hold is made for some system checks. Then the pump drive turbines are switched to nuclear steam and runup to full 3600 rpm speed for vibration checks. Finally, power ascension begins, to be completed in a day or two.

During all this time the sampling system is operating and tracing the crud level. Figures 10 through 15 show startup crud bursts of various magnitudes. Before pump speed increase the trace is uninterpretable for reasons noted in subsection 2. At the time of pump speed increases the crud trace breaks, shooting upward in a linear fashion towards another break corresponding to establishment of full flow in the primary loop. Subsequently the trace executes an apparent two-exponential-term decay much like the power drop event described in subsection 1. The resemblence is not perfect, for there is some distortion of the shape on the approach to maximum, as a rule. The size of the crud burst in general is variable but is by far the largest type of transient of all; a maximum crud level of 6.5 ppm was observed on one occasion. Eventually, if reactor operation allows, the crud level decays back down to a steady state value. The activities involved in pump runup, establishment of full flow, and power ascension are clearly indicated by the concurrent hot leg cold leg temperature traces and are unmistakably correlated with the features of the trace as described.

FIGURE 10

STARTUP CRUD BURST 2/17/80

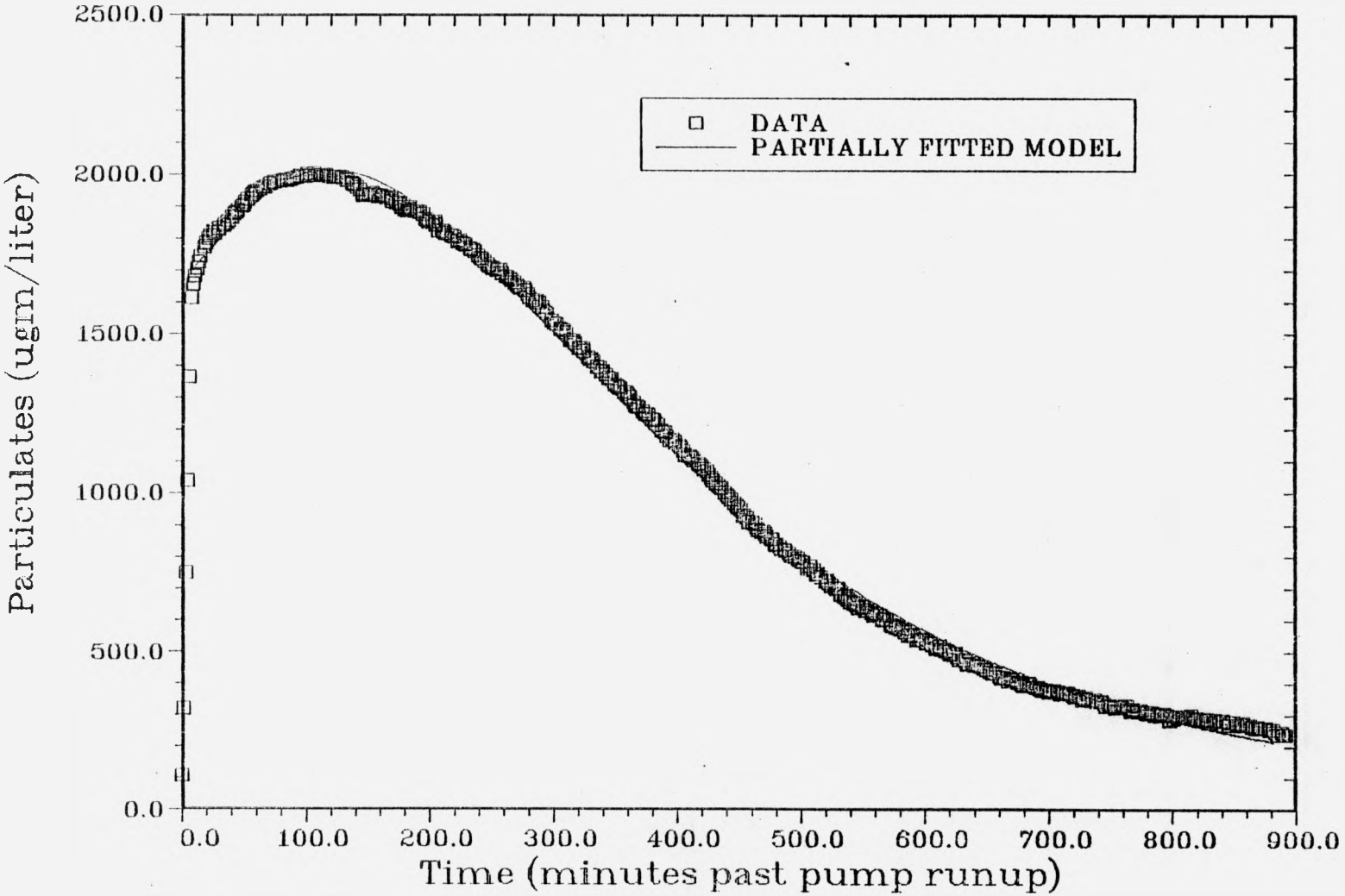

FIGURE 11

STARTUP CRUD BURST 4/13/81

(data peak is off scale)

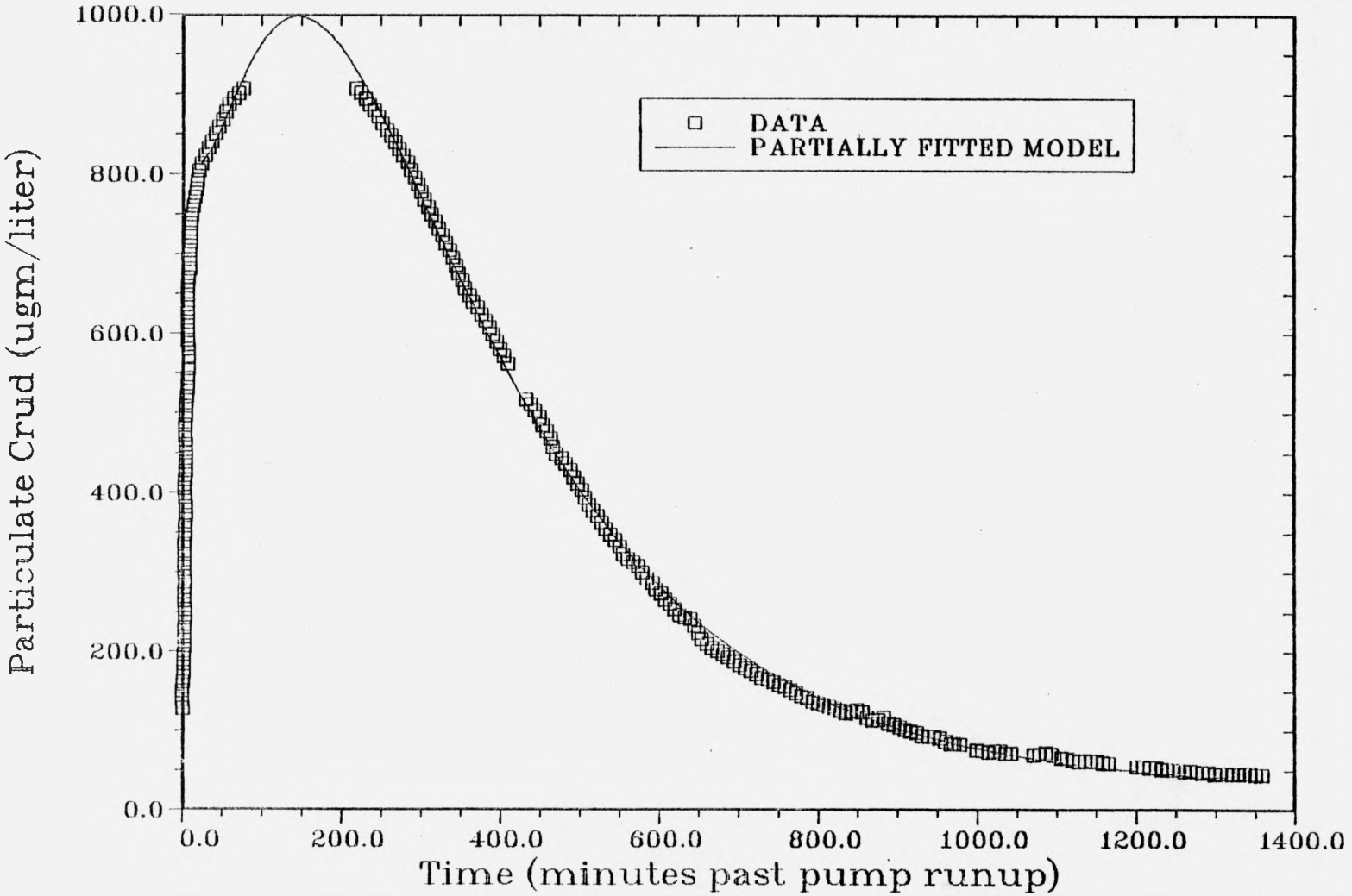

FIGURE 12

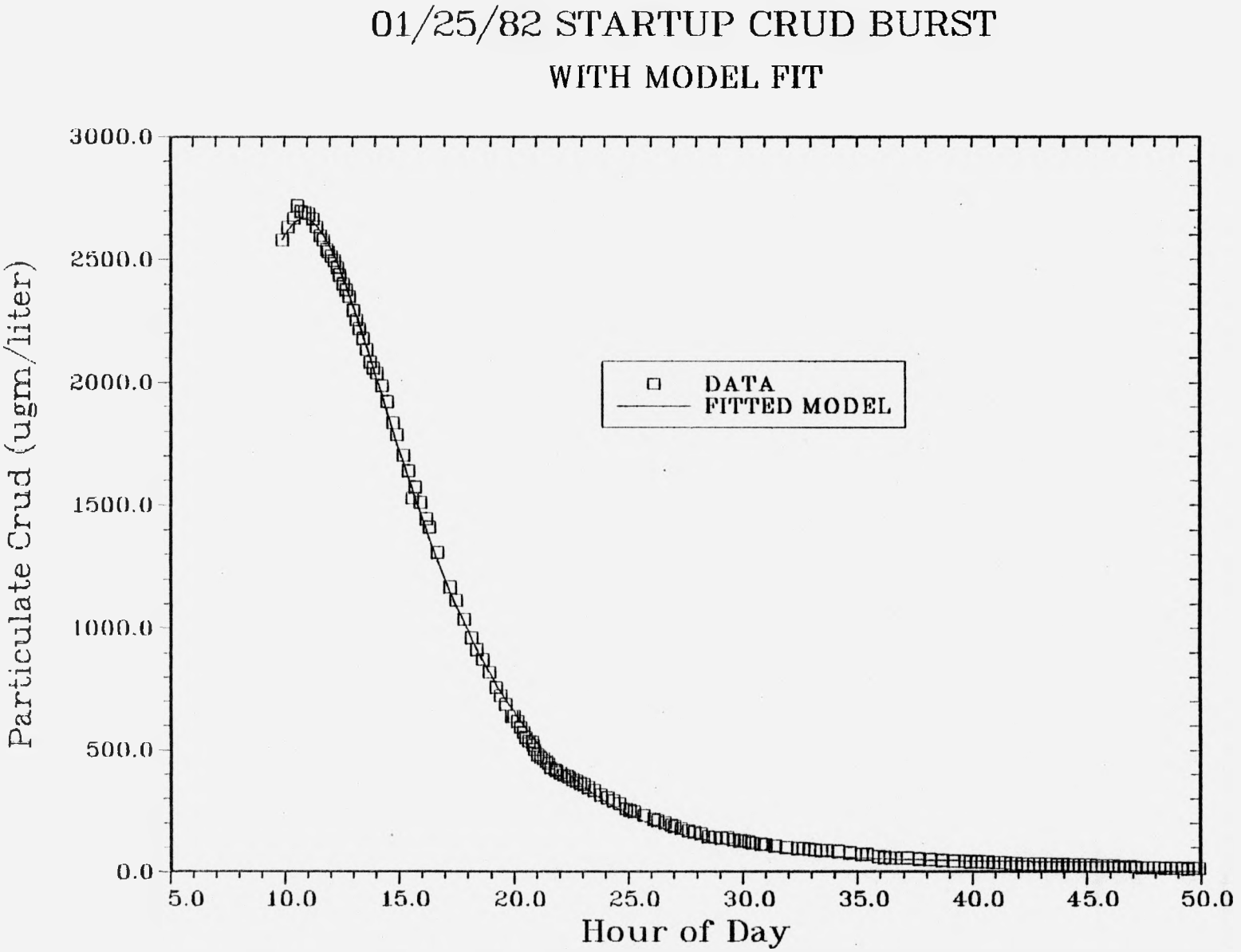
01/25/82 STARTUP CRUD BURST
WITH MODEL FIT
Particulate Crud (ugm/liter)
3000.0
2500.0
2000.0
1500.0
1000.0
500.0
0.0
5.0
10.0
15.0
20.0
25.0
30.0
35.0
40.0
45.0
50.0
Hour of Day
DATA
FITTED MODEL

FIGURE 13

STARTUP CRUD BURST 4/15/82

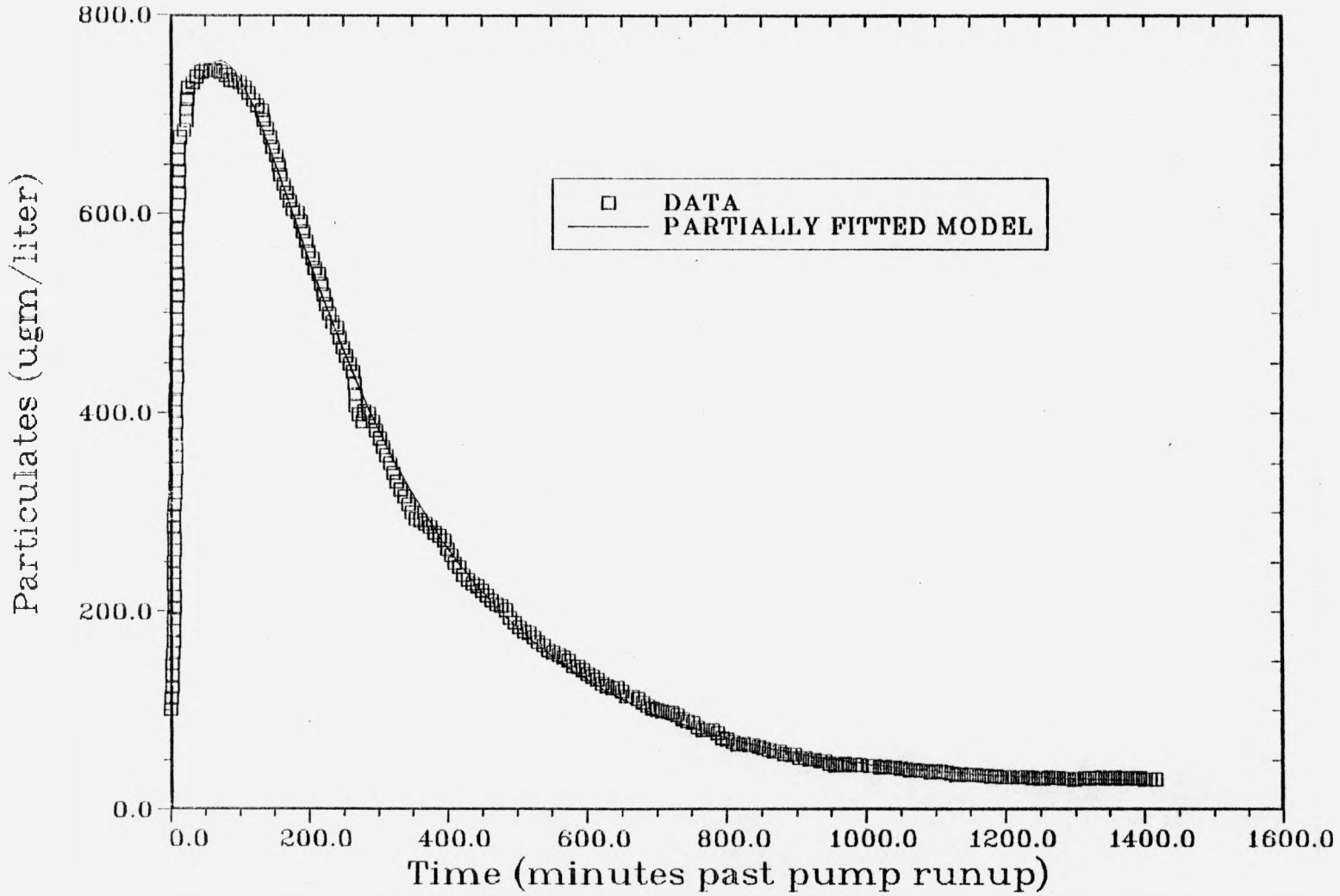

FIGURE 14

STARTUP CRUD BURST 11/3/82

(data peak is off scale)

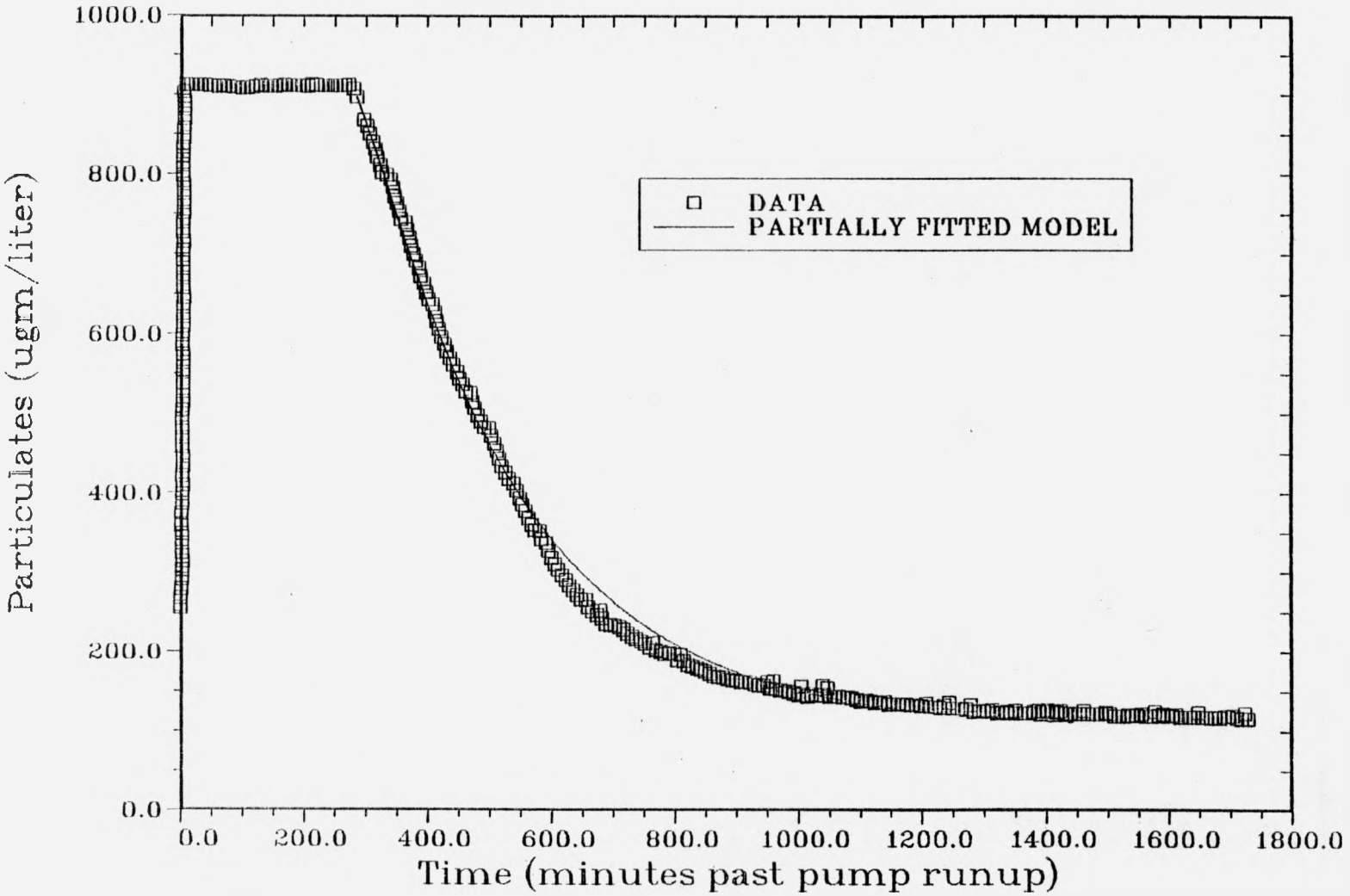

FIGURE 15

STARTUP CRUD BURST 11/10/82

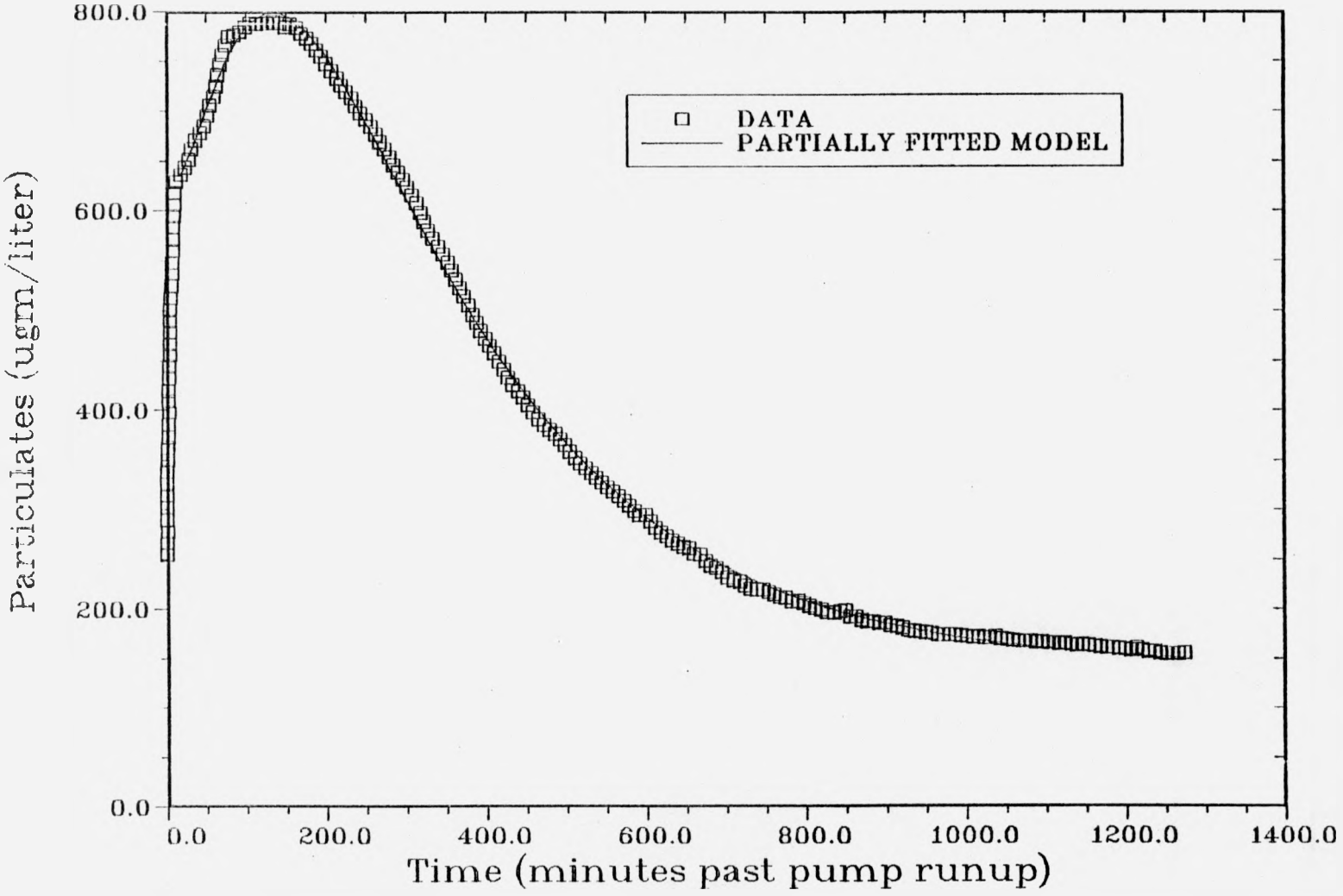

Apparently what is happening in terms of crud behavior in all startup cases is that a large amount of loose crud has been generated by the previous shutdown and any primary loop maintenance that occurred in the interim. Also, the corrosion product begins to turn towards brown, oxidized rust in the oxidizing environment of a cold shutdown. The runup of primary pumps stirs up and resuspends this loose material, whereupon it is supplemented by resuspension of partially adherent crud from the piping walls until that supply runs short and the mechanisms of crud loss take over. There may be some adjustments of crud morphology back to the high-temperature reduced form from the enormous physico-chemical perturbation of a shutdown and cold layup. As in the power drop crud burst described in subsection 1., power rises do not seem to add anything detectable to this strong crud resuspension.

Incidently, the small bump in the trace at 325 minutes in Figure 13, and the increase in slope evident at 60 minutes in Figure 15 are the result of the two chemical events mentioned at the beginning of Section B.

C. Detailed Analysis of Crud Transients

The general features of the various types of crud bursts described above together with their correlation against known reactor events leads us naturally to the notion that the transport of particulate crud may be described by a simple, stirred-tank, first-order model of exchange among a few states. For conceptual simplicity this modeling is done on a volume basis, not coolant mass basis, so we convert the measurement data by noting the average primary coolant density--0.8072 kg/dm^3.

The assumptions used to model the crud transients and extract the kinetic parameters consist of:

a) The primary loop is a stired tank of volume V = 628897 dm^3, (calculated from plant drawings), and surface area 3.35326 x 10^6 dm^2. Allowance has been made for deadlegs, of which there are several, and 5-cell operation (N Reactor has 6 steam generator cells, but only 5 are normally in service). Total primary loop letdown flow q_{LD} = 3892 dm^3/min at average coolant temperature, a number which has held reasonably constant over the time span covering the crud transients of interest.

b) Particulate crud in the coolant has concentration PC ($\mu gm/dm^3$); it may be lost to letdown with rate constant, q_{LD}/V, (1/min), or plate out onto piping walls with rate constant, a, (1/min). This plated-out crud is loosely adherent, concentration, L, ($\mu gm/dm^2$), so defined because it is susceptible to re-suspension by the coolant flow with characteristic rate constant, b, (1/min).

c) In the lack of power disturbances, the loosely adherent crud can slowly "sinter" together to join an already present and limitless tightly adherent crud on the walls with rate constant, c_T, (1/min).

d) When reactor power decreases the tightly adherent crud transfers to the loosely adherent state at a rate, R_L, ($\mu gm/dm^2$/min). When starting up, there exists an R_L as well, but it is assumed due to a relaxation of the crud chemistry/morphology back to high temperature reducing conditions. Therefore this startup R_L diminishes with time.

e) When operating, there is a steady formation of suspended crud derived from both a contribution from the crud in makeup feed water and a thermal-cycle-magnetite-solubility-difference mechanism. Together these contributions result in a constant rate of of formation of suspended crud, R_{PC}, ($\mu gm/dm^3$/min).

The exchange states described by the preceding model may be summed up by the following diagram:

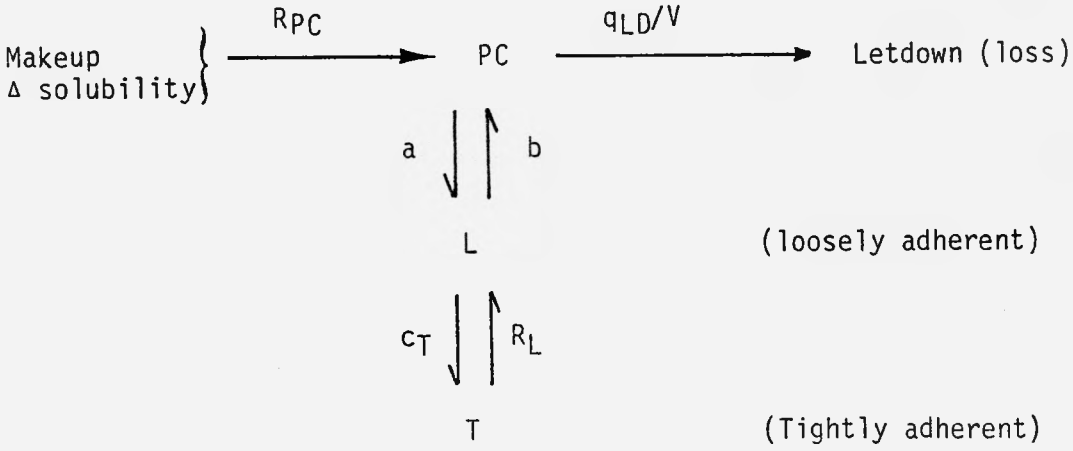

And of course the resulting system of linear, first order differential equations with constant coefficients defined by the model is

$$\frac{dL}{dt} = -(b+c_T)L + a\frac{V}{S}\,PC + R_L \qquad (7)$$

$$\frac{dPC}{dt} = \frac{S}{V}\,bL \;-(a + \frac{q_{LD}}{V})\,PC + R_{PC} \qquad (8)$$

Only the treatment of R_L changes in fitting the model to the several types of crud transients. This is due partly to the lock-step uniformity of standard reactor operating practice.

The above model was used to explain/fit each type of crud transient with appropriate treatment of R_L and appropriate choice of which of the other parameters a, b, c_T, R_{PC} were to be adjusted. The model was then fit to the crud transients using the same non-linear least squares fitting computer program in Reference 8, but with a few modifications. One handy feature of this program is that it can fit models in differential form; the program may be directed to integrate a system of differential equations with initial conditions by a 4th order Runge-Kutta solver and minimize the integrated sum-of-squares. This feature was used in most of the fits.

1. Power Drop Crud Transient Detailed Analysis

Before a time t_{start}, the model is in its steady state with $R_L = 0$. After t_{start} the power drops at a constant rate giving rise to a non-zero R_L adjustable parameter. After a time t_{stop}, R_L is again zero and no more loosely adherent crud is generated from tightly adherent crud. The parameters R_{PC}, a, b, c_T and R_L were adjusted to fit the model to the data with the choice of time to match the power drop. In this fit, the integrated form of the model was used, which is:

$$PC = \frac{a_3L^\circ + (\lambda_1-a_1)PC^\circ + \frac{\lambda_1-a_1}{a_2\lambda_1}[a_2R_{PC} - (\lambda_2-a_1)R_L]}{\beta} \exp[\lambda_1\Delta t]$$

$$+ \frac{- a_3L^\circ - (\lambda_2-a_1)PC^\circ - \frac{\lambda_2-a_1}{a_2\lambda_2}[a_2R_{PC} - (\lambda_1-a_1)R_L]}{\beta} \exp[\lambda_2\Delta t]$$

$$+ PC^\infty \qquad (9)$$

and,

$$L = \frac{- (\lambda_2-a_1)L^\circ + a_2PC^\circ \quad \frac{a_2R_{PC} - (\lambda_2-a_1)R_L}{\lambda_1}}{\beta} \exp[\lambda_1\Delta t]$$

$$+ \frac{(\lambda_1-a_1)L^\circ - a_2PC^\circ - \frac{a_2R_{PC} - (\lambda_1-a_1)R_L}{\lambda_2}}{\beta} \exp[\lambda_2\Delta t]$$

$$+ L^\infty \qquad (10)$$

where,

$$PC^{\infty} = \frac{a_3 R_L - a_1 R_{PC}}{\lambda_1 \lambda_2}, \qquad L^{\infty} = \frac{a_2 R_{PC} - a_4 R_L}{\lambda_1 \lambda_2}$$

and, (11)

$$\lambda_1 = \frac{a_1 + a_4 + \beta}{2}, \qquad \lambda_2 = \frac{a_1 + a_4 - \beta}{2},$$

$$\beta = \sqrt{(a_1 - a_4)^2 + 4 a_2 a_3},$$

$$a_1 = -(b + c_T), \qquad a_2 = a \frac{V}{S}, \tag{12}$$

$$a_3 = \frac{S}{V} b, \qquad a_4 = \left(a + \frac{q_L D}{V}\right)$$

Note the two-exponential-term form of equation (9). Before the power ramp, $t < t_{start}$ and clearly we have $PC = PC^{\infty}$ and $L = L^{\infty}$, with $R_L = 0$. During the power ramp, R_L becomes finite, and $\Delta t = t - t_{start}$. The initial conditions L° and PC° equal L and PC at t_{start}. Finally, after the power ramp, $R_L = 0$ once again, and now $\Delta t = t - t_{stop}$. PC° and L° likewise become PC and L at t_{stop}. Note that the values of PC^{∞} and L^{∞} are affected by the value of R_L.

The resulting parameters of the fit are displayed in Table 1, where the uncertainties are the estimated standard deviations of the parameters. The parameter c_L, discussed in the next section, was derived from R_L and the known rate of power drop. The fitted function is displayed in Figure 6.

Five parameters is as much a parameterization as a functional form like equation (9) can support. As such, there is a coupling between the choice of values for each of the

TABLE 1. PARTICULATE CRUD TRANSIENT MODEL FITTING RESULTS

Transient	a ($\frac{1}{min}$)	b ($\frac{1}{min}$)	c_T ($\frac{1}{min}$)	c_L ($\frac{\mu gm}{dm^2 MW}$)	R_L ($\frac{\mu gm}{dm^2 min}$)	R_L° ($\frac{\mu gm}{dm^2 min}$)	k ($\frac{1}{min}$)	R_{PC} ($\frac{\mu gm}{dm^3 min}$)	C° ($\frac{\mu gm}{dm^3}$)	L° ($\frac{\mu gm}{dm^2}$)
power drop 3/26/80	1.252E-2 ±5.7E-4	2.724E-3 ±2.8E-4	3.697E-3 ±8.0E-5	0.445 (derived)	24.01 ±1.1			0.5653 ±0.028		
shutdown 2/8/80	fixed at 1.252E-2	fixed at 2.724E-3	fixed at 3.697E-3	0.6594 ±0.0017	48.51 (derived)			1.094		
shutdown 3/1/80	fixed at 1.252E-2	fixed at 2.724E-3	fixed at 3.697E-3	0.3402 ±0.0018	19.03 (derived)			0.7861		
shutdown 5/13/80	fixed at 1.252E-2	fixed at 2.724E-3	fixed at 3.697E-3	0.4577 ±0.0068	33.92 (derived)			1.886		
startup 2/17/80	fixed at 1.252E-2	fixed at 2.724E-3	fixed at 3.697E-3			20.35 ±0.34	8.485E-3 ±1.0E-4	fixed at 0.5653	1711.	2445. ±18.
startup 4/13/81	fixed at 1.252E-2	fixed at 2.724E-3	fixed at 3.697E-3			13.17 ±0.29	1.058E-2 ±1.9E-4	0.3659 ±0.016	813.7	1087. ±12.
startup 1/25/82	fixed at 1.252E-2	fixed at 2.724E-3	fixed at 3.697E-3			17.37 ±0.49	7.093E-3 ±1.5E-4	fixed at 0.5653	2579.	3493. ±30.
startup 4/15/82	fixed at 1.252E-2	fixed at 2.724E-3	fixed at 3.697E-3			19.90 ±7.4	6.417E-2 ±1.1E-2	0.3423 ±0.092	727.0	862.4 ±56.
startup 11/3/82 (tail)	fixed at 1.252E-2	fixed at 2.724E-3	fixed at 3.697E-3					1.408 ±0.016 (tail)	897.6 (tail)	914.9 ±5.3 (tail)
startup 11/10/82	fixed at 1.252E-2	fixed at 2.724E-3	fixed at 3.697E-3			9.751 ±0.23	1.293E-2 ±2.6E-4	1.887 ±0.011	636.1	796.3 ±90.

parameters. The parameters b and c_T, especially were negatively coupled. This means that nearly as good a fit could be obtained if b were raised and c_T were lowered, or vice versa. This stands to reason, since both parameters contribute to the loss of crud from suspension. More certain values of b and c_T could be obtained if one could have measured L during the crud burst and fitted its data simultaneously. This idea, however, evokes formidable experimental difficulties.

Attempts to include the ensuing upward power ramps into the model for this crud transient were done in a straightforward manner but were unsuccessful; the fit could not be equaled and therefore it was concluded that the power rises did not contribute to the transient.

Equally unfruitful were attempts to verify the values S/V and q_{LD}/V. They of course over-paramaterized the model, and so had to be left to "known" values.

2. Normal Shutdown Crud Transient Detailed Analysis

Here it is presumed by the crud traces of Figures 7, 8 and 9 that the system is at steady state with $R_L = 0$ until the standard downward power ramp starts. At this time R_L is switched on to remain to the end of the trace.

For these fits, the slight variation in power ramps among the three transients examined was handled by decomposing R_L into a coefficient c_L ($\mu gm/dm^2/MW$), times the rate of power loss dP/dt (Mw/min):

$$R_L = c_L \left| \frac{dP}{dt} \right| \tag{13}$$

The quantity dP/dt was entered into the fitting program in the form of a simple interpolator between entries in the Console Log, thus taking care of "switching on" R_L at the right moment.

These fits were also done with the differential forms of the model as in equations (7) and (8), in order to avoid the integration and coding involved with the integral form.

Initial fits were tried with three parameters; b, c_L, and R_{PC}. Very good fits were had, since three parameters is the limit for the form of the crud traces. There was very strong parameter coupling between b and c_L, furthermore, with b much higher than as determined in the power drop. The result was that b would be selected very high, c_L relatively low, and R_{PC} clearly chosen to miss the baseline in order to compensate for slight deficienceies in the fit on the ramp. This is not really fair, and since the normal shutdown is merely the long-time analogue of the power drop, it was decided to fix b at the value so determined there, select for R_{PC} a value which coincided with the steady state baseline by eye and fit only one parameter--c_L. All other parameters were fixed at values found for the power drop, whereupon a successful fit would demonstrate consistency the model with the power drop.

The one-parameter fits were successful, albeit with a slight lag in "getting moving" as shown in Figures 7, 8 and 9. The parameter so determined is listed in Table 1. The value selected by eye for R_{PC} is also listed for each shutdown, as well as an average R_L derived from c_L and the known dP/dt. The agreement between the fited c_L for the normal shutdowns with the derived c_L for the power drop is gratifying, and indicates that the postulated generation of loosely adherent crud from protective, tightly adherent crud is indeed proportional to the rate of power drop, despite some variation in power rates among the four cases.

3. Startup Crud Transient Detailed Analysis

The unfortunate thing about startup crud burst model fittings is that there is no previous state that easily characterizes PC° and L°, like the steady state which preceded the power

drop. The general shape of the functional form of the data still limits us to 5 parameters, and so a complete fit of a, b, c_T, R_L, R_{PC}, PC° and L° is out of the question. Rather, we must again fix a, b and c_T to values determined by the power drop fit and deal with R_L, R_{PC}, PC° and L° as adjustable parameters.

Considering the general features and operational conditions of a startup, it was concluded that the rapid linear rise of crud level was not produced by the same erosion of loosely adherent crud that dominates after the runup is completed. Instead, it is postulated that the previous shutdown and relaxation towards oxidized morphology together have produced a very large amount of crud which has merely fallen out of suspension in the stagnant water. The pump runup stirs this crud back into suspension, hence the rapid, linear rise in suspended crud level which begins and ends so closely with the beginning and attainment of full flow. The remaining rise of crud level towards maximum is attributed to the erosion of loosely adherent crud.

One might expect a good fit could be attained without any R_L from the point of full flow onwards, which is tantamount to a pure two-exponential-term decay functional form. It turns out that this is not the general case; fits of that sort have been tried on several of the transients shown in Figures 10 through 15 with poor results. It appears that an additional boost in loosely adherent crud is required for a while in a form not mimicked by merely increasing L° at the start of the fit. The simplest way to meet this requirement is to give R_L the functional form

$$R_L = R_L^\circ e^{-kt} \qquad (14)$$

where k is a time constant with units (1/min). The sort of mechanistic justification for this fudge lies in postulating

that the shocked and oxidized crud is now relaxing back to magnetite and is temporarily breaking up in doing so. There is no regular power rise at the attainment of full flow in startups which can be assigned responsibility for generating loose crud, and in fact no power rise anywhere in these studies has been linked to an increase or inception of a crud transient. A shutdown is an enormous perturber of piping crud, with the thermal shock and change in chemical environment. Some sort of change upon reestablishment of operating environment which is otherwise missed on small power perturbations may be possible.

To treat the startup crud transient then, no attempt is made to fit the transient before full flow was attained. At this point, R_L is given the functional form of equation (14) with two adjustable parameters; $R°_L$ and k. A value of PC° is selected by eye to match the data and L° becomes another adjustable parameter. R_{PC} is either fixed at the value determined for the power drop, or made an adjustable parameter, when there was not any obvious problem with baseline drift in the turbidimeter. All other parameters in the differential model of equations (7) and (8) were fixed at values determined by the power drop fit. The one exception to this procedure is the transient shown in Figure 14, where only the tail was available for modeling. Here, it was felt that R_L has effectively decayed away, and so R_L was set to zero for the fit.

The resulting fits, shown in Figures 10-15, indicate good consistency with the power drop model as long as Equation (14) is used. The fitted or selected parameters are shown in Table 1. The fitted values for $R°_L$ seem to be fairly consistent, as are the time constants k. The variability in PC° and L° are understandable in terms of the (unknown) extent of primary loop maintenance, water chemistry control, shutdown

time, etc., during each outage which act to create suspendable crud.

The variability of R_{PC} is noticeable too. This represents the steady running crud level, and is therefore a rather important parameter. Several reasons may contribute to its variability; including zero problems with the turbidimeter (steady running is usually below 10% of full scale on the low scale) or variations in makeup water quality and system pH. As yet no correlations have been made.

D. Crud Level Transient Analysis General Discussion

In this report, it has been discussed that the particulate corrosion products in the N Reactor primary loop consist of magnetite particles of a fairly uniform log normal distribution centered about 1-2 microns which probably does not change much as the reactor goes through its operating cycles. Furthermore, the transients that are seen in the coolant may be rationalized fairly consistently in terms of a simple stirred-tank model linking makeup and loss to loosely adherent and tightly adherent crud. We are forced to accept this many states, for the non-instantaneous buildup of crud during transients can not be explained with fewer. The N Reactor primary loop surfaces, due to its large carbon steel surface area, present only corrosion product to the coolant; the only very notable exception is the fuel surfaces themselves, where the cladding in all but the extreme inlet side of the pressure tubes is bare of corrosion product. Elsewhere on the piping walls the corrosion product coverage is complete. It has been noted that the variation of suspended crud on startup is easily explained, and that at least possibilities exist for rationalizing the generation of more loose crud in early stages of startup; the innards of the primary loop on shutdown can be observed to slowly take on a brownish tinge during an outage.

Some of the more fundamental assumptions regarding the model should now be discussed. The matter of suspended crud loss usually begs the question whether the letdown loss is really as large as assumed, or if there is a substantial, unacknowledged contribution from crud traps. N Reactor has over 2000 valves of 1 1/2" or larger in line with, or connected to, the primary loop, as well as approxiately 74,000 dm^3 of deadlegs. Some well known crud traps are the pressure tube outlet nozzle caps, which have to be flushed of accumulated crud on a regular basis. There must be some contribution from crud traps, and some of the letdown leakage must consist of steam leakage from valve stem seals; the problem is how to partition these contributions. It would be desirable to be able to do so, since crud traps constitute a major source of personnel exposure, but it appears for now that one must presume the crud trap buildup rate is proportional to the suspended crud level. In the very near future, N Reactor will undertake to reinject its failed fuel detection streams, thus causing a major drop in q_{LD}/V. The changes in crud transients under this new mode of operation would help answer the question.

A single stirred tank model forces the modeler to accept a single surface-to-volume ratio, unless he wishes to evoke exchanges between separate tanks in order to reflect the varying flow conditions within a PWR primary loop. If he does, then he needs more data to fit that model, or some plausible way to relate the observed crud transients at one point to those at another. If he does not, then he must accept the fact that his kinetic parameters determined from the simplest model are some sort of average of a possibly wide range over the entire loop. This presents problems when comparing kinetic results with other determinations at other installations. However, if all that is needed is a description of the situation at his own installation, the direct measurement is sufficient and the kinetic parameters are a convenient, phenomenological way to store the information.

The quantity R_{PC} is an important one, for it represents the steady state crud level in the coolant. Up to now R_{PC} has not been decomposed in the fitting processes, there has only been some discussion as to its possible sources. With no prior knowledge it is arbitrary whether one treats the baseline sources as a formation of crud in the coolant or as a steady erosion of crud from the walls, perhaps driven by base metal corrosion. In the present case, this could be handled by giving R_L some small, baseline value to represent the loosening of excess protective base corrosion product layer. Though there may be some contribution by this means, it is at odds with the stabilizing tendency of our hydrothermal "sintering" mechanism. Instead, the base metal corrosion contribution may be more simply and quantifiably added to R_{PC} through a magnetite solubility mechanism.

To support the R_{PC} role, an ongoing program of makeup water purity evaluation has produced one preliminary result of 27 $\mu gm/dm^3$ magnetically filterable crud in the makeup water (at average reactor coolant temperature). Noting that at steady state (with $R_L = 0$),

$$R_{PC} = \frac{(a + \frac{q_{LD}}{V})(b + c_T) - ab}{(b + c_T)} \; PC^{\infty} \qquad (15)$$

we can see that the median of all filter sample ppm determinations, 50.15 x .8072 = 40.48 $\mu gm/dm^3$ is equivalent to R_{PC} = 0.542 $\mu gm/dm^3/min$. The contribution from 27 $\mu gm/dm^3$ in the makeup stream would be 27 x q_{LD}/V = 0.167 $\mu gm/dm^3/min$, leaving 0.542 - 0.167 = 0.375 $\mu gm/dm^3/min$ to be accounted for.

N Reactor primary loop pH is controlled between 9.8 and 10.4 by means of ammonia. Typically the pH at 25°C is found to be 10.0 - 10.3 pH units. Some calculations made of the solubility of magnetite based on the data of Sweeton and Baes,[12] the base dissociation constant of ammonia[13] and acid dissociation constant of water[14] showed that the maximum solubility transport and reformation of crud in the N Reactor PCL could vary from zero to 0.544 $\mu gm/dm^3/min$ over this pH range. To be plausible this

solubility transport rate must be matched serially in steady state by corrosion of the primary loop hot leg or cold leg carbon steel surfaces. Coupon tests of carbon steel corrosion in the primary loop of 15 years' duration show uniform corrosion rates of 0.01 to 0.1 mil per year. Noting that one half of the primary loop's carbon steel surface area is 6.5×10^5 dm^2, and that the reactor operates 180 days of the year on the average, we find the corrosion available to supply the solubility mechanism to be 0.11 to 1.1 $\mu gm/.dm^3/min$. This is sufficient to supply the full range of possible solubility transport, which itself is sufficient to account for the remainder (0.375) of R_{PC}.

Soon a production test will be undertaken to raise the pH of the primary loop by 0.2-0.3 units. It should be very interesting in this context to see if there is a long-term impact on PC^{∞} as a result.

We turn now to some comparisons of the results described so far with those of others reported in the literature. The most direct comparison should be with Reference 9, where the S/V ratio of the Winfrith reactor, the equilibrium crud levels, and the particle size distribution all are similar. There is the caveat that the Winfrith is a BWR, having a more oxidized form of iron oxide crud. Reference 9 deals with crud transients from power ramps, Powdex filter changeouts (not applicable to N Reactor) and chemistry changes. An explicit differential source term for the crud in the bursts (which have the same shape as those observed here) is avoided by the authors, as is the mechanism for producing it. No re-suspension mechanism is considered either. However, a deposition coefficient, k_d, having the units of velocity, is derived and presented. It ranges from 1×10^{-3} to 3×10^{-3} cm/sec for a variety of particle size ranges and transient types. The constant "a" determined here, when multiplied by V/S and converted to appropriate units, yields $k_d = 3.91 \times 10^{-4}$ cm/sec, which is a factor of 4 to 10 lower. This is not too bad,

considering the possiblity of different flow conditions within each reactor. For example, N Reactor's primary loop (besides deadlegs) has flow Reynold's numbers that vary from 885,000 to 4.7×10^7. It is not clear how to average this kind of situation for comparisons to other work. One possible way which may be of no significance whatever is to weight average the Reynolds's number by the time spent in that flow condition as the coolant courses around the loop. At N Reactor this number comes to 2.17×10^7. The Reynold's number is often used to correlate particulate deposition rates, but exactly which number to use in comparing reactor primary systems is problematical.

Deposition rates determined under less comparable conditions are to be found in Reference 15. There, a water-magnetite slurry was injected through 3.5 and 5 mm tubes for a very few seconds, temperatures being less than the boiling point. A correlation of a mass-based deposition coefficient with Reynold's number was made, indicating roughly a first-power dependence for deposition onto Zr-4 tubing. Converting to units of dm/min, this correspondence works out to 0.006 dm/min at 10^5 Reynold's number, 0.06 dm/min at 10^6, and (extrapolated) 0.6 and dm/min at 10^7. The k_d at N Reactor in equivalent units is 0.00235 dm/min. In addition, Reference 15 found that deposition rates were apparently linear with slurry concentration below 400 ppm; a tacit assumption on the model considered here.

Finally, with some effort, a comparison can be made with Reference 16, a laudable experimental examination of magnetite deposition in a 5.6 mm tube at high temperature conditions. There were 8 experiments made under turbulent isothermal conditions, all but three of them, however, supercritical. The data consisted of total buildup of magnetite from a constant 1-2 ppm suspension on the tube wall against time as determined by counting the activated chromium in the slurry with a GeLi detector spectroscopy system. Most runs were for 4 hours, with three going to 40 hours, none of which could produce complete coverage.

The authors of reference 16 interpreted the buildup curves to be due to a time dependent deposition with no resuspension; resulting in a logarithmic-rise functional form. They found a good, linear correlation of initial buildup rate with Reynold's number.

In order to compare the results of reference 16, a re-interpretation of the data must be made in terms of the present model. A tube that starts with no deposit at all will build up loosely adherent crud L and tightly adherent crud T as described by the following equations:

$$\frac{dL}{dt} = -(b + c_T)L + a\frac{V}{S} PC \tag{16}$$

$$\frac{dT}{dT} = c_T L \tag{17}$$

in terms of the present model, noting that PC is now a constant. This system can be easily integrated to give, when $T^\circ = L^\circ = 0$,

$$L = \frac{k_D PC}{b+c_T} \left[1 - e^{-(b+c_T)t}\right] \tag{18}$$

$$T = c_T \frac{k_D PC}{b+c_T} t + c_T \frac{k_D PC}{(b+c_T)^2} \left[1 - e^{-(b+c_T)t}\right] \tag{19}$$

where we substitute $k_D = aV/S$. However, the quantity which is measured is actually L + T, and so we have

$$L + T = \frac{k_D PC}{b+c_T}\left[c_T t + \left(\frac{c_T}{b+c_T} + 1\right)\left(1 - e^{-(b+c_T)t}\right)\right] \tag{20}$$

The functional form predicted by equation (20) is significantly different from the one in Reference 16 only at long times, when the term in t dominates.

The data from all 8 experiments were individually digitized off the published figures and fit to equation (20) with three adjustable parameters, k_D, b and c_T. A typical fit of a long term run, experiment 7, is depicted in Figure 16. Fits to all eight experiments appear to be as good as those in the reference. The parametric results are displayed in Table 2, which can be viewed as an extension of Table 1 in the reference. Also in Table 2 are estimated values of the laminar sublayer thickness z_{ls} and the wall shear stress R_w[17] for each experiment. In the N Reactor primary loop z_{ls} ranges from 29-152 microns, and R_w from 69-207 Nwt/m^2.

As expected, the fitted k_D values corresponded closely with the initial buildup rates found in the reference in all but one case, and therefore had the same linear correlation with Reynold's number. However, the comparison with the N Reactor k_D is poor, the latter being 0.00235 dm/min in comparable units. The comparison with the N Reactor b fares a little better, that being 0.00272 1/min. The c_T value was difficult to obtain reliably, and compares poorly with the N Reactor value of 0.00370 1/min. One should note that the temperatures of experiments 1, 2 and 3 corresponded roughly with the N Reactor primary system. All other experiments were supercritical.

Why the k_D values compare so poorly with N Reactor is an open question but may be due to as-yet undiscovered dependencies of deposition on tube size. Perhaps the situation at low fractional coverage is greatly different than at full crud coverage. In any case, the problem of deciding exactly how to compare an overall system parameter to one determined under carefully defined flow condition remains.

FIGURE 16

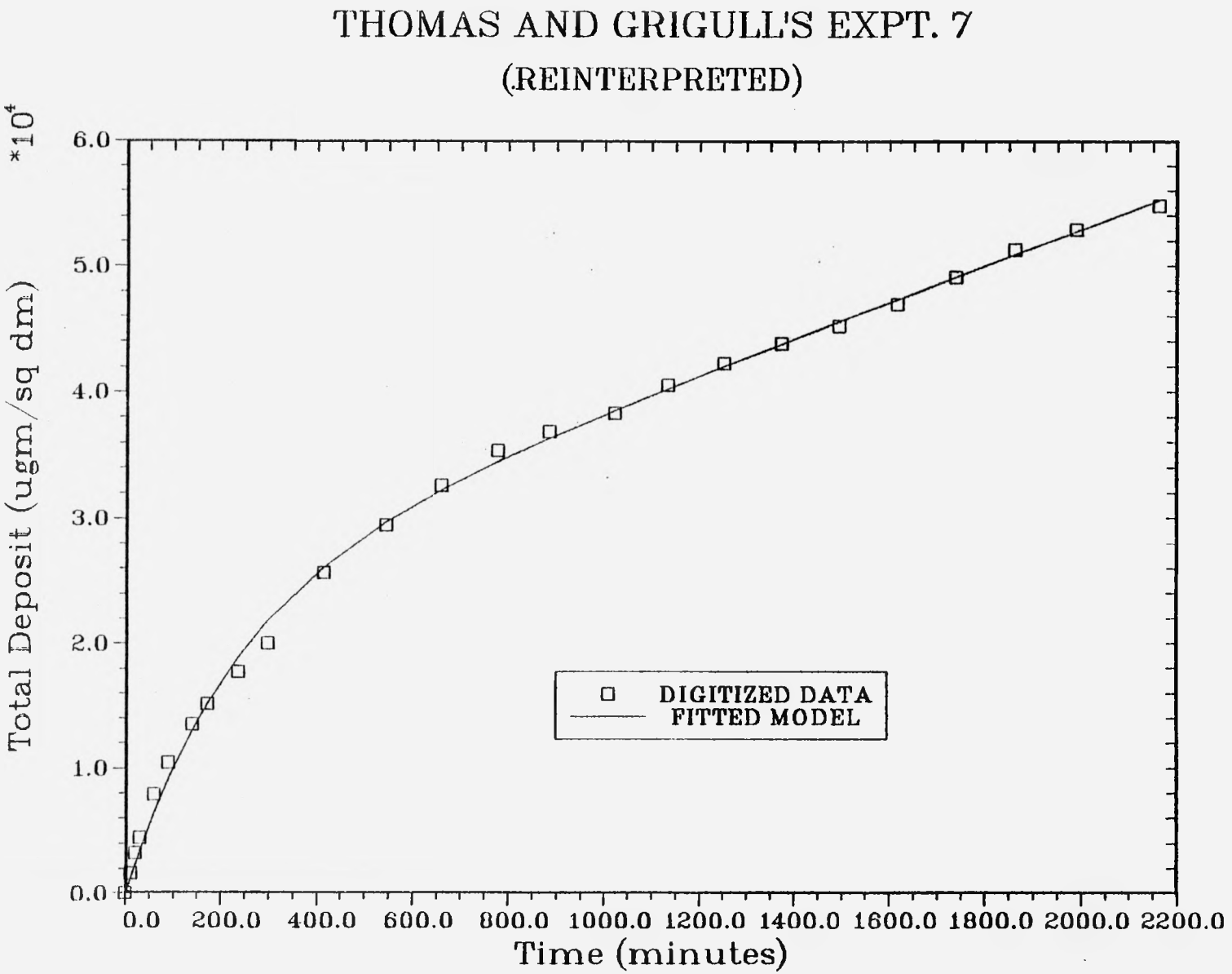

TABLE 2. RESULTS OF PRESENT MODEL FIT TO THOMAS AND GRIGULL'S DATA

Experiment #	Reynolds #	k_D (dm/min)	b (1/min)	c_T (1/min)	$z_{ls}^{\dagger}$ (microns)	$R_w^{\ddagger}$ (Nwt/m^2)
1	3.75 E+4	0.0221 ± 0.0017	0.01102 ± 0.0024	0.0007017 ± 0.0012	51.2	5.6
2	4.58 E+4	0.03992 ± 0.0024	0.01128 ± 0.0020	0.0007144 ± 0.0011	46.2	2.4
3	7.70 E+4	0.07432 ± 0.0017	0.02043 ± 0.0011	0.002905 ± 0.00036	35.7	5.9
4	1.04 E+5	0.1409 ± 0.0079	0.004326 ± 0.00039	0.0004388 ± 0.000042	30.7	4.8
5	1.40 E+5	0.9093 ± 0.038	0.007333 ± 0.0014	0.0003108 ± 0.0015	26.5	14.0
6	1.55 E+5	0.3404 ± 0.0049	0.01268 ± 0.00068	0.002559 ± 0.00050	25.1	10.1
7	1.81 E+5	0.3488 ± 0.014	0.003869 ± 0.00027	0.0005293 ± 0.000038	23.2	13.1
8	1.82 E+5	0.9409 ± 0.096	0.00742 ± 0.0013	0.0006980 ± 0.000085	23.2	17.3

*D. Thomas und U. Grigull,"Experimentelle Untersuchung über die Ablagerung von suspendiertem Magnetit bei Rohrströmungen in Dampferzeugern", Brennst.-Wärme-Kraft 26, (1974) Nr. 3, März, p. 109-115.

† Estimated Laminar Sublayer Thickness.

‡ Estimated Wall Shear Stress.

And it is indeed a problem, for what we really want to know for future source term analysis is the detailed deposition/erosion behavior of particulates in each and every flow condition in the reactor primary system--not just some overall average. We come away from these literature comparisons unassured that the means exists as yet to deconvolute the section-by-section deposition coefficient from the overall average measurement combined with the individual section Reynold's numbers. The average behavior is adequate for the present purpose of estimating the necessary capacity of a magnetic filter and predicting its effects on crud inventories. However a filter's quantitative effect on the source term will depend on the deposition rate of particulates on fuel surfaces, which may be described by a coefficient quite different than our "loop-average" value.

VI. PARTICULATE CRUD SIMULATION MODEL

A. Rationale

One of the near term goals of the program activities that produced this report is the development of a simulation model of particulate crud transport. The reason is severalfold. The particulate crud that is in suspension is felt to have a fairly direct role in the source term of corrosion product activation, and hence an early understanding of it will aid in sorting out the expected total production of certain nuclides for the purposes of various studies. Secondly, a separate program at N Reactor to install a magnetic filter on a primary loop bypass required some predictive ability of its effect on particulate crud levels for conceptual design purposes. Thirdly, efforts to lessen the total loop letdown and raise the loop pH are soon to be underway, and a baseline understanding of particulate crud transport to compare with their results was desired.

The model developed in this report serves as a predictor of the fate of particulate crud as a function of let down flow, run time, bypass filter flow, etc., with the appropriate parameters. To include the effect of a bypass magnetic filter, one merely needs to replace q_{LD} in Equations (7) and (8) with

$$q = q_{LD} + q_{EMF} \times e_{EMF} \tag{21}$$

where q_{EMF} is the magnetic filter bypass flow and e_{EMF} is the efficiency of the filter. To decompose R_{PC} into the separate contributions discussed in Section V., one uses

$$R_{PC} = R_{CS} + \frac{q_{LD}}{V} \; PC_{MU} \tag{22}$$

where R_{CS} is the solubility mechanism term and PC_{MU} is the suspended crud level in the makeup.

To simulate the particulate crud transport of a typical N Reactor operating cycle, one recognizes that the cycle consists of a startup, a run for some period of time, and a shutdown. Fortunately the startup and shutdown operations are fairly consistent, and the crud transients associated with them have a reproducible functional form. Therefore, one merely has to simulate a startup, then a run and finally a shutdown with Equations (7) and (8) to comprise the model. This means beginning the simulation with a startup PC° and L° and "switching on" a startup R_L. It will decay off to a steady state for the extent of the run. At the end of the run, switch R_L to a constant shutdown quantity for the one hour's duration of the shutdown.

B. Parameter Selection

There is variability in the startup and shutdown crud bursts, as we have seen, and also in the steady state R_{CS}. To make one universal simulation, then, there has to be an averaging of appropriate parameter values. For the simulation model then, the value used for PC° is the average of five found in Table 1, or 1293.36 μgm/dm^3. For L° it is likewise 1736.71 μgm/dm^2. For the startup $R°_L$, the average of 5; 16.11 μgm/dm^2/min is used. However, the average of only 4 values of k; 0.009770 1/min, is used, since one value seemed anamolously high.

The values to use for R_{CS} and PC_{MU} are those discussed in Section V., namely 0.375 μgm/dm^3/min and 27.0 μgm/dm^3, respectively. They were selected to give R_{PC} the value 0.542 μgm/dm^3/min, equivalent to the median of filter sample crud level determinations. This was used rather than the average of the fitted or selected R_{PC} values in Table 1 because it was trusted more; the latter values are prone to instrumental zero drift and/or vagaries in the fitting process.

The shutdown power ramps vary somewhat in slope in an unpredictable fashion. The best thing to do is once again average them. The most direct way is to average the fitted-or-derived R_L values of Table 1, rather than averaging both c_T and dP/dt and using the product. Thus a shutdown R_L value of 31.37 $\mu gm/dm^2/min$ was arrived at.

Finally, the values a and b from Table 1 were used as is, since only one independent determination of them has been made to date.

C. Coding, Input and Output

Based on the necessary equations and parameters, the simulation model was developed. A listing of this short program is provided in the Appendix. The method used is to solve equations (7), (8), (21) and (22) by a Runge-Kutta solver, since the system is not stiff. For the ease of a direct comparison, the simulation is run with the magnetic filter operating, and without, simultaneously.

The input to the computer program is in namelist format (NAMELIST/ INPUT/) and includes TRUN, the length of reactor operating cycle in days, QLD, the letdown flow in gpm, QEMF, the filter bypass flow in gpm, and EEMF, the filter efficiency.

The program solves the equations starting with PC° and L° and the startup R_L for 10 minute intervals with and without the magnetic filter until a steady state is reached. It then extends the time intervals until the value TRUN is exceeded, whereupon it switches R_L to the shutdown value and does six more 10 minute intervals. There is tabular output of integrated quantities for each time interval.

The output table consists of 15 quantities; time (minutes) and 7 quantities each for the cases with and without the magnetic filter.

The description of the seven quantities is as follows:

Heading	Quantity (unit conversions not shown)
GRAMS LOOSE =	$L \times S$
GRAMS MOBILE =	$PC \times V$
GRAMS IN =	$\int_o^t PC_{MU} \times q_{LD} \times d\tau$
GRAMS FORMED =	$\int_o^t R_{CS} \times V \times d\tau$
GRAMS TO EMF =	$\int_o^t q_{EMF} \times e_{EMF} \times PC \times d\tau$
GRAMS TO CRIB = (letdown)	$\int_o^t q_{LD} \times PC \times d\tau$
GRAMS TO WALL =	$\int_o^t S \times [a \times V/S \times PC - b \times L] \times d\tau$

The last quantity is equal to the net change in L and T, $\Delta(L+T)$ since time zero, and is often negative.

The final activity of the program is to generate a plot of PC versus time for the simulation. Figure 17 is such a plot for TRUN = 5 days, QLD = 500 gpm, QEMF = 4000 gpm and EEFM = 100 percent.

D. Usage and Discussion

The simulation model has been used to size a magnetic filter for project presentation and for studies of its effect on filterable radionuclide transport in conjunction with reductions in letdown flow. The median measures of the five main activation product radionuclide filterable mass specific activities determined so far from 138 filter samples are as follows:

SUSPENDED CRUD VS TIME

FIGURE 17

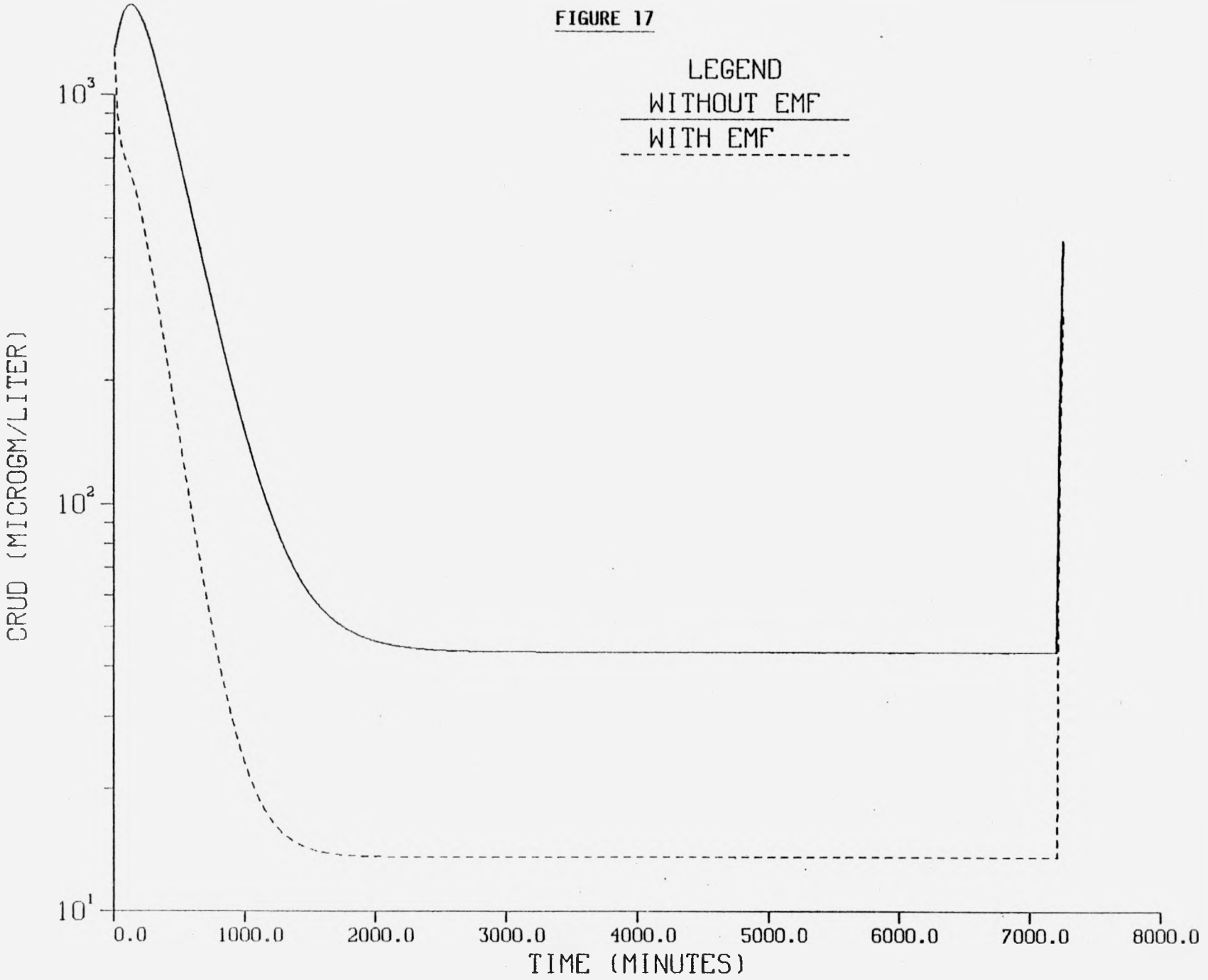

NUCLIDE	MEDIAN FILTERABLE MASS SPECIFIC ACTIVITY (mCi/gm)
Fe^{59}	1.29
Co^{60}	0.838
Zr^{95}	0.569
Cr^{51}	0.387
Mn^{54}	0.370
Co^{58}	0.154

These may be multiplied by the grams of crud transported to various locations to give an approximation to radioactivity transport by particulates. The listing of the program in the Appendix shows that the model parameters are present in DATA statements. The program will consequently simulate the average, "typical" particulate transport over the operating cycle unless some of the parameter values are changed. It is conceivable that simulations starting with different values of PC° may be desirable, for example. The necessary coding changes are relatively simple.

The use of the code with the currently selected parameters predicts a significant net total loss of crud from piping walls for all but very extended runs, i.e., the startup and shutdown crud loosening mechanisms are not made up for an extended length of time. This is not necessarily a paradox, for on a reactor average basis we may take the view that the tightly adherent crud is limitless because of replenishment by corrosion.

At present the connection between particulate transport and the source term of activated corrosion product radionuclide production is not developed. The observations of crud deposits on discharged N Reactor fuel, when coupled with solubility calculations of magnetite in ammoniated waters suggest that the activation mechanism proposed by Burrill[18,19,20] is directly applicable. This being so, and if a steady state between particulate deposition and dissolution is reached rapidly, then the source term should be proportional to the steady suspended crud level. A magnetic filter, then, should lessen the source term by the same amount it depresses PC^{∞}. Work is ongoing and planned to develop these ideas.

VII. CONCLUSIONS

A. The levels of particulate crud in the N Reactor primary loop are high enough to measure by filtration and have been established for equilibrium operation and for reactor transients. The crud approximates magnetite in composition.

B. The particle size distribution of the crud during equilibrium operation has been established sufficiently to account for the filterable mass of crud. It has been shown to be unchanging in distribution under equilibrium operation, and literature suggests this remains true during transients in crud levels.

C. An auto-correcting turbidimetric instrument provides a stable, convenient method to continuously monitor crud levels in primary coolant, and has a linear response to at least 6 ppm.

D. Crud transients are caused to the greatest extent by decreases in power. Chemical events normally do not cause detectable crud level transients, except while major transients are already occurring. Power rises do not cause crud transients.

E. Particulate crud transport at N Reactor can be modeled simply by stirred-tank exchange between coolant, loosely adherent crud on the walls, and tightly adherent crud. Loose crud may be generated from adherent crud by decreases in power and, upon reactor startups, by some sort of morphological relaxation to high-temperature conditions.

VIII. ACKNOWLEDGEMENTS

The author wishes to thank those technicians, Joanne Perkins, Karen Sprow, Steve Burke, Bryan Carlson and Maryanne Kummerer, who, at differing times, performed indispensible and valuable work collecting and reducing the data upon which this report is based, often under less than ideal working conditions.

IX. REFERENCES

1. W. E. Berry and R. B. Diegle, "Survey of Corrosion Product Generation, Transport and Deposition in Light Water Nuclear Reactors", EPRI-NP-522, March, 1979.

2. British Nuclear Energy Society, "Water Chemistry of Nuclear Reactor Systems", Proceedings of the Bournemouth Conference, 24-27 October 1977, BNES, London, England, 1978.

3. British Nuclear Energy Society, "Water Chemistry of Nuclear Reactor Systems 2", Proceedings of the Bournemouth Conference, 14-17 October 1980, BNES, London, England, 1981.

4. B. B. Emory, "Production Test N-425, Activated Corrosion Products (CRUD) Behavior Study", UNI-757, April 13, 1977.

5. B. B. Emory, "Theoretical Considerations in the Design of Crud Sample Systems for Nuclear Power Plants", UNI-SA-55, September 25, 1978. Presented at the NACE Corrosion '79 Corrosion Product Sampling Symposium, Atlanta, Georgia, March 12-16, 1979.

6. B. B. Emory and D. B. Bechtold, "Activated Corrosion Products (CRUD) Behavior Study, Interim Report No. 1", UNI-893, December 13, 1977.

7.

8. J. L. Dye and V. A. Nicely, "A General Purpose Curvefitting Program for Class and Research Use", J. Chem, Ed. 48, 443. July, 1971. Some minor modifications have been made to have the program calculate the equivalent diameters from the channel settings and calculate the specific mass and specific area.

9. F. A. Means, R. S. Rodliffe, and K. Harding, "An Investigation of Particulate Corrosion Product Transients in the Primary Coolant of the Winfrith Steam Generating Heavy Water Reactor", Nuclear Technology 47, 385, March, 1980.

10. F. A. Means, "The Formation and Breakup of Corrosion Product Agglomerates in the Primary Coolant of Water Reactors", CEGB-RD/B/N 4268, 1978.

11. J. RozenberG, H. Kahan and L. Dollé, "In Pile Loop Water Chemistry Analytical and Sampling Techniques.", Paper 16 of Reference 2, p. 151.

12. F. H. Sweeton and C. F. Baes, Jr., "The Solubility of Magnetite and Hydrolysis of Ferrous Ion in Aqueous Solutions at Elevated Temperatures", J. Chem. Thermodynamics, 2, 479, (1970).

13. B. F. Hitch and R. E. Mesmer, "The Ionization of Aqueous Ammonia to 300°C. in KCl Media, J. Sol. Chem. 5 (10), 667, (1976).

14. R. H. Busey and R. E. Mesmer, "The Ionization of Water in KCl Media to 300°C.", J. Sol. Chem. 5 (2), 147, (1976).

15. K. A. Burrill, "The Deposition of Magnetite Particles from High Velocity Water onto Isothermal Tubes:, AECL-5308, February, 1977.

16. D. Thomas and U. Grigull, "Experimentelle Untersuchung über die Ablagerung von suspendiertem Magnetit bei Rohrstömungen in Dampferzeugern", Brennst.-Warme-Kraft 2 (3), 109, (March, 1974).

17. F. A. Holland, Fluid Flow for Chemical Engineers, Chemical Publishing Co., Inc. New York, 1974, p. 16-38.

18. K. A. Burrill, "Corrosion Product Transport in Water-Cooled Nuclear Reactors. Part I: Pressurized Water Operation", Can. J. Chemical Engineering 55, 54, (1977).

19. K.A. Burrill, "Corrosion Product Transport in Water-Cooled Nuclear Reactors. Part II: Boiling Water with Direct Cycle Operation", Can. J. Chem. Eng. 56, 79, (1978).

20. K.A. Burrill, "Corrosion Product Transport in Water-Cooled Nuclear Reactors. Part III: Boiling Water with Indirect Cycle Operation", Can. J. Chem. Eng. 57, 211 (1979).

APPENDIX

SOURCE LISTING OF PARTICULATE CRUD SIMULATION MODEL CRUDFILT

```
@R CRUDFILT.MAIN
READ-ONLY MODE
CASE UPPER ASSUMED
ED 16R1-WED-01/11/84-14:03:19-(1,)
ED,T
0:
      1:C          H A N F O R D  N  R E A C T O R
      2:C          P A R T I C U L A T E  C R U D  S I M U L A T O R
      3:C          A N D
      4:C          M A G N E T I C  F I L T E R  C O M P A R A T O R.
      5:C          MAIN ROUTINE.  SIMULATES OBSERVED PARTICULATE CRUD BEHAVIOR
      6:C          IN HANFORD N REACTOR PRIMARY LOOP FROM STARTUP THROUGH RUNNING
      7:C          AND NORMAL SHUTDOWN.  DOES THE SAME FOR THE SAME SYSTEM WITH
      8:C          A BYPASS MAGNETIC FILTER IN OPERATION FOR THE PURPOSES OF
      9:C          DIRECT COMPARISON.
     10:C               FOR DOCUMENTATION CONSULT:  UNI-TR-9, AVAILABLE
     11:C                                          FROM THE NTIS,
     12:C                                          IMSL, INC. EDITION  9 LIBRARY,
     13:C                                          ISSCO,INC. DISSPLA VERSION 9,
     14:C                                          SPERRY UNIVAC FORTRAN FIN LEV. 10
     15:C          PURPOSE:  TO ASSESS CRUD REMOVAL CAPABILITY OF VARIOUS SIZES
     16:C                    OF MAGNETIC FILTER FROM HANFORD N REACTOR PRIMARY
     17:C                    COOLANT, PIPE WALLS AND CRIB.
     18:C          METHOD:  RUNGE-KUTTA SOLUTION OF TWO ORDINARY 1ST ORDER LINEAR
     19:C                   DIFFERENTIAL EQUATIONS EMPLOYING IMSL, INC. SUBROUTINE
     20:C                   DVERK.  OUTPUT DETAILED LIST OF VALUES FOR THE
     21:C                   CHOSEN LENGTH OF RUN, LETDOWN FLOW RATE,
     22:C                   FILTER FLOW, EFFICIENCY.
     23:C          INPUT:  NAMELIST/INPUT/QLD,QEMF,EEMF,TRUN
     24:C                  WHERE QLD = PCL LETDOWN FLOW IN GPM,
     25:C                        QEMF = BYPASS FILTER FLOW IN GPM,
     26:C                        EEMF = FILTER EFFICIENCY IN PERCENT,
     27:C                        TRUN = LENGTH OF REACTOP RUN IN DAYS.
     28:C          OUTPUT:  TITLE, ECHO OF INPUT, TIME SERIES TABLE OF
     29:C                   VARIABLES OF INTEREST, WITH AND WITHOUT FILTER,
     30:C                   132 COLUMNS, 57 LINES PER PAGE,
     31:C                   ISSCO, INC. DISSPLA PLOT OF SUSPENDED CRUD LEVEL
     32:C                   VS TIME WITH AND WITHOUT FILTER.
     33:C
     34:C
     35:C
     36:CCCCC      FUNCTION PARTIC CONTAINS EQUATION SYSTEM TO BE SOLVED.
     37:           EXTERNAL PARTIC
     38:           REAL K,L,LEMF,LO
     39:CCCCC      DISSPLA PLOTTING ARRAYS
     40:           DIMENSION IPKRAY(200), EXTRME(4)
     41:CCCCC      ARRAYS FOR IMSL, INC. DVERK TO SOLVE DIFF. EQNS.
     42:           DIMENSION Y(2),C(24),W(2,9)
     43:CCCCC      ARRAYS FOR STORING CALCULATED TIME SERIES DATA.
     44:CCCCC      PRINCIPAL VARIABLES:  L = LOOSELY ADHERENT CRUD
     45:CCCCC      ON PIPE WALLS, UGM/DM**2, PC = PARTICULATES IN
     46:CCCCC      COOLANT, UGM/DM**3.  ALSO CORRESPONDING VARIABLES
     47:CCCCC      IN PRESENCE OF MAG. FILTER.
     48:           DIMENSION L(1000),LEMF(1000),PC(1000),PCEMF(1000),TIME(1000),
     49:     2     ISTOPV(1000)
     50:CCCCC      COMMUNICATE RATE CONSTANTS AND FORCING CONSTANTS TO
     51:CCCCC      FUNCTION  PARTIC TO CHARACTERIZE MIXED-TANK BEHAVIOR
```

```
52:CCCCC      OF CRUD IN PCL.
53:           COMMON /PARAM/A,B,CT,RCS,PCMU,S,V,RLOU,RLOD,K
54:CCCCC      COMMUNICATE INPUTTED VALUES TO FUNCTION PARTIC
55:           COMMON /VAR/QEM,EEMF,QLD,ISTOP
56:           NAMELIST/INPUT/QLD,QEMF,EEMF,TRUN
57:CCCCC      LOAD EQUATION SOLVING PARAMETERS FOR DVERK
58:           DATA N,NW,IND,IER,TOL/2,2,1,0,1.E-6/
59:CCCCC      LOAD RATE CONSTANTS AND OTHER PARAMETERS
60:           DATA A,B,CT,RCS,PCMU,S,V,RLOU,RLOD,K,LO,PCO,TSS
61:      2    /1.252462E-2,2.723927E-3,3.697196E-3,0.375,27.0,
62:      3    3.3532E6,.28897.,16.11,31.37,0.009770,1736.71,1293.36,
63:      4    3000./
64:           WRITE(6,100)
65:  100 FORMAT('1','H A N F O R D  N - R E A C T O R  P A R T I C U',
66:      2    'L A T E  C R U D  S I M U L A T O R'/'0',
67:      3    30X,'A N D'/'0',
68:      4    'M A G N E T I C  F I L T E R  C O M P A R A T O R'///
69:      5    1X,'DOCUMENTATION TO BE FOUND IN UNI-TR-9, AVAILABLE',
70:      2    ' FROM THE NTIS')
71:           READ(5,INPUT)
72:           WRITE(6,200) TRUN,QLD,QEMF,EEMF
73:  200      FORMAT(////1X,'INPUTTED PARAMETERS ARE:'/'0',
74:      2    'LENGTH OF RUN = ',1PE11.3,' DAYS'/'0',
75:      3    'PCL LET-DOWN FLOW = '1PE11.3,' GPM'/'0',
76:      4    'MAGNETIC FILTER FLOW =',1PE11.3,' GPM'/'0',
77:      5    'MAGNETIC FILTER EFFICIENCY = ',1PE11.3,' PER CENT')
78:CCCCC      CONVERT TIME TO MINUTES
79:           TRUN = TRUN*1440.
80:CCCCC      CONVERT FLOWS TO LITERS/MIN
81:           QLD = QLD*3.78541
82:           QEMF = QEMF*3.78541
83:CCCCC      CONVERT QLD TO OPERATING TEMPERATURE EQUIVALENT
84:           QLD = QLD/0.8072
85:CCCCC      CONVERT PER CENT TO FRACTIONAL
86:           EEMF = EEMF/100.
87:CCCCC      TABLE HEADINGS
88:           WRITE(6,300)
89:  300      FORMAT('1','TIME (MIN)',5X,'GRAMS LOOSE',4X,'GRAMS MOBILE',
90:      2     6X,'GRAMS IN',4X,'GRAMS FORMED',3X,
91:     3'GRAMS TO EMF',3X,'GRAMS TO CRIB',2X,'GMS TO WALL')
92:CCCCC      BEGIN INITIALIZATION AND LOGIC TO SELECT
93:CCCCC      APPROPRIATE TIME POINTS FOR TABULATION OF OUTPUT.
94:CCCCC      IN GENERAL, MAKE TEN-MINUTE INTERVALS UNTIL REACH TSS
95:CCCCC      OR END-OF-RUN.  AT END-OF-RUN, SWITCH ON SHUTDOWN MODE (ISTOP)
96:CCCC       AND DO SIX MORE INTERVALS.  IF REACH TSS FIRST
97:CCCCC      (STEADY STATE), MAKE ONLY 100 MORE (LONGER) INTERVALS
98:CCCCC      UNTIL END-OF-RUN TO SAVE COMPUTATION.  LOAD TIME AND
99:CCCCC      STOP SWITCH VECTORS APPROPRIATELY.
100:          X = 0.
101:          XSTEP = 10.
102:          ISTOP = 0
103:          INDEX = 1
104:   10     CONTINUE
105:          TIME(INDEX) = X
106:          ISTOPV(INDEX) = ISTOP
107:          XEND = X+XSTEP
108:          IF(XEND.GT.TRUN) THEN
```

```
109:            ISTOP = 1
110:            XSTEP = 10.
111:            DO 50 J=1,6
112:            XEND = X+XSTEP
113:            X = XEND
114:            INDEX = INDEX+1
115:            TIME(INDEX) = X
116:            ISTOPV(INDEX) = ISTOP
117:     50     CONTINUE
118:            GO TO 1000
119:            ELSE IF(XEND.GT.TSS.AND.XEND.LE.TRUN.AND.
120:       2    (TRUN-TSS)/100..GT.10.) THEN
121:            ISTOP = 0
122:            XSTEP = (TRUN-TSS)/100.
123:            ELSE
124:            END IF
125:            XEND = X+XSTEP
126:            X = XEND
127:            INDEX = INDEX+1
128:            GO TO 10
129:  1000      CONTINUE
130:CCCCC       INITIALIZE ALL NECESSARY VALUES TO CORRESPOND
131:CCCCC       TO TIME(1) = 0.
132:CCCCC       ALSO SET NO. OF POINTS TO CALCULATE/PLOT
133:            NPNTS = INDEX
134:            L(1) = LO
135:            PC(1) = PC0
136:            LEMF(1) = LO
137:            PCEMF(1) = PC0
138:            GL = LO*S/1.E6
139:            GM = PC0*V/1.E6
140:            GI=0.
141:            GF = 0.
142:            GTF = 0.
143:            GTC = 0.
144:            GTW = 0.
145:            GLEMF = GL
146:            GMEMF = GM
147:            GIEMF = 0.
148:            GFEMF = 0.
149:            GTFEMF = 0.
150:            GTCEMF = 0.
151:            GTWEMF = 0.
152:CCCCC       WRITE INITIAL VALUES
153:            J = 1
154:            WRITE(6,400) TIME(J),GL,GM,GI,GF,GTF,GTC,GTW,
155:       2    GLEMF,GMEMF,GIEMF,GFEMF,GTFEMF,GTCEMF,GTWEMF
156:   400      FORMAT(///1X,54X,'WITHOUT MAGNETIC FILTER'/
157:       2    1X,7(1PE11.3,4X),1PE11.3/
158:       3    1X,57X,'WITH MAGNETIC FILTER'/
159:       4    1X,15X,6(1PE11.3,4X),1PE11.3)
160:CCCCC       KEEP TRACK OF OUTPUT ENTRIES -- MAX OF 8 PER PAGE
161:            IENTRY = 1
162:CCCCC       CALCULATE AND OUTPUT VALUES FOR TIME POINTS
163:            DO 40 J=2,NPNTS
164:CCCCC       SET UP IMSL, INC. DVERK ARGUEMENTS
165:            X = TIME(J-1)
```

```
166:            XEND = TIME(J)
167:            Y(1) = L(J-1)
168:            Y(2) = PC(J-1)
169:            QEM = 0.
170:            ISTOP = ISTOPV(J-1)
171:            IND = 1
172:            CALL DVERK(N,PARTIC,X,Y,XEND,TOL,IND,C,NW,W,IER)
173:CCCCC       LOOSE CRUD AND PARTICULATE (MOBILE) CRUD
174:            L(J) = Y(1)
175:            PC(J) = Y(2)
176:CCCCC       NOW DO SAME FOR FILTER CASE
177:            QEM = QEMF
178:            X = TIME(J-1)
179:            XEND = TIME(J)
180:            Y(1) = LEMF(J-1)
181:            Y(2) = PCEMF(J-1)
182:            ISTOP = ISTOPV(J-1)
183:            IND = 1
184:CCCCC       IMSL, INC. SUBROUTINE DVERK CALCULATES NEW Y(1), Y(2)
185:            CALL DVERK(N,PARTIC,X,Y,XEND,TOL,IND,C,NW,W,IER)
186:            LEMF(J) = Y(1)
187:            PCEMF(J) = Y(2)
188:CCCCC       UNIT CONVERSIONS TO GRAMS, KNOWING SURFACE AREA (S) AND
189:CCCCC       VOLUME (V) OF PCL.
190:CCCCC       ALSO CALCULATE SOME DESIRED CRUD FLUXES TO FILTER,ETC.
191:            DT = TIME(J)-TIME(J-1)
192:            GL = L(J)*S/1.E6
193:            GM = PC(J)*V/1.E6
194:            GI = GI+QLD/1.E6*DT*PCMU
195:            GF = GF+RCS*V*DT/1.E6
196:            GTF = 0.
197:            GTC = GTC+QLD*DT/1.E6*(PC(J-1)+PC(J))/2.
198:            GTW = GTW+DT/1.E6*S*(A*V/S*(PC(J-1)+PC(J))/2.
199:     2      -B*(L(J-1)+L(J))/2.)
200:            GLEMF = LEMF(J)*S/1.E6
201:            GMEMF = PCEMF(J)*V/1.E6
202:            GIEMF = GI
203:            GFEMF = GF
204:            GTFEMF = GTFEMF+QEMF*EEMF*DT/1.E6*(PCEMF(J-1)+PCEMF(J))/2.
205:            GTCEMF = GTCEMF+QLD*DT/1.E6*(PCEMF(J-1)+PCEMF(J))/2.
206:            GTWEMF = GTWEMF+DT/1.E6*S*(A*V/S*(PCEMF(J-1)+PCEMF(J))/2.
207:     2      -B*(LEMF(J-1)+LEMF(J))/2.)
208:CCCCC       START A NEW PAGE IF 8 ENTRIES ALREADY ON PAGE
209:            IF (IENTRY.GE.8) THEN
210:            WRITE(6,300)
211:            IENTRY = 0
212:            END IF
213:            WRITE(6,400) TIME(J),GL,GM,GI,GF,GTF,GTC,GTW,
214:     2      GLEMF,GMEMF,GIEMF,GFEMF,GTFEMF,GTCEMF,GTWEMF
215:            IENTRY = IENTRY + 1
216:   40       CONTINUE
217:CCCCC       CALCULATIONS FINISHED, MAKE THE DISSPLA PLOT
218:            CALL USMNMX(TIME,NPNTS,1,XLO,XHI)
219:            CALL USMNMX(PC,NPNTS,1,EXTRME(1),EXTRME(2))
220:            CALL USMNMX(PCEMF,NPNTS,1,EXTRME(3),EXTRME(4))
221:            CALL USMNMX(EXTRME,4,1,YLO,YHI)
222:            CALL VRSTEC
```

```
223:            CALL PAGE(11.,8.5)
224:            CALL AXSPLT(XLO,XHI,9.5,XORIG,XSTP,XAXIS)
225:            CALL TITLE('SUSPENDED CRUD VS TIME$',100,
226:           2'TIME (MINUTES)$',100,
227:           3'CRUD (MICROGM/LITER)$',100,XAXIS,6.5)
228:            CALL YAXANG(0.)
229:            MAXLIN = LINEST(IPKRAY,200,12)
230:            CALL LINESP(2.0)
231:            CALL LINES('WITHOUT EMF$',IPKRAY,1)
232:            CALL LINES('WITH EMF$',IPKRAY,2)
233:            DX = XLEGND(IPKRAY,2)
234:            DY = YLEGND(IPKRAY,2)
235:            XPOS = 9.5/2.-DX/2.
236:            YPOS = 6.5-DY
237:            YCYCLE = 6.5/ALOG10(YHI/YLO)
238:            CALL YLOG(XORIG,XSTP,YLO,YCYCLE)
239:            CALL BLNK1(XPOS,9.5/2.+DX/2.,YPOS,6.5,0)
240:            CALL LEGLIN
241:            CALL CURVE(TIME,PC,NPNTS,0)
242:            CALL DASH
243:            CALL CURVE(TIME,PCEMF,NPNTS,0)
244:            CALL RESET('BLNKS')
245:            CALL LEGEND(IPKRAY,2,XPOS,YPOS)
246:            CALL ENDPL(-1)
247:            CALL DONEPL(0)
248:            STOP
249:            END
EOF:249
0:
```

```
@ER CRUDFILT.PARTIC
NO CORRECTIONS APPLIED.
READ-ONLY MODE
CASE UPPER ASSUMED
ED 16P1-WED-01/11/84-14:03:34-(0,)
EDIT
0:
     1:            SUBROUTINE PARTIC(N,X,Y,YPRIME)
     2:CCCCC       FOR USE BY IMSL ROUTINE DVERK
     3:CCCCC       DOCUMENTATION IN UNI-TR-9, AVAILABLE FROM THE NTIS,
     4:CCCCC       AND IMSL, INC. EDITION  9 LIBRARY.
     5:CCCCC       EVALUATES DIFFERENTIAL MODEL OF PARTICULATE CRUD
     6:CCCCC       DVERK CALLED BY MAIN ROUTINE "MAIN", SIMULATING
     7:CCCCC       PARTICULATE TRANSPORT AT HANFORD N REACTOR
     8:CCCCC       A STIRRED TANK, WITH CRUD EXISTING AS MOBILE (IN COOLANT)
     9:CCCCC       CRUD (UGM/DM**3), LOOSE (ON WALLS) CRUD (UGM/DM**2), AND
    10:CCCCC       TIGHTLY ADHERENT CRUD. CRUD SOURCES ARE IN FROM MAKEUP
    11:CCCCC        FLOW = LETDOWN FLOW QLD (DM**3/MIN) CONTAINING PCMU
    12:CCCCC       (UGM/DM**3) CRUD, FROM SOLUBILITY DIFFERENCE FORMATION
    13:CCCCC       = RCS (UGM/DM**3/MIN), AND FROM TIGHT STATE BY STARTUP
    14:CCCCC       OR SHUTDOWN LOOSENING FUNCTION RL (UGM/DM**2/MIN).
    15:CCCCC        CRUD SINKS ARE TO FILTER THROUGH FILTER FLOW QEMF, TO
    16:CCCCC       LETDOWN FLOW AND BACK TO TIGHT STATE FROM LOOSE.
    17:CCCCC       PERMITTED EXCHANGES ARE IN-AND-FORMED -> MOBILE -> LETDOWN,
    18:CCCCC       MOBILE -> FILTER, MOBILE <-> LOOSE AND LOOSE <-> TIGHT.
    19:CCCCC       CERTAIN EXCHANGES ARE SWITCHED ON OR OFF AT RIGHT TIMES.
    20:CCCCC       PARAMETERS ARE:
    21:CCCCC       QLD = LETDOWN FLOW, DM**3/MIN
    22:CCCCC       QEMF = FILTER FLOW, DM**3/MIN
    23:CCCCC       EEMF = FILTER EFFICIENCY, FRACTIONAL
    24:CCCCC       ISTOP = SHUTDOWN "SWITCH"
    25:CCCCC       S = PCL SURFACE AREA,DM**2
    26:CCCCC       V = PCL VOLUME, DM**3
    27:CCCCC       RLOU = INITIAL STARTUP LOOSENING FUNCTION, UGM/DM**2/MIN
    28:CCCCC       K = STARTUP LOOSENING DECAY CONSTANT, 1/MIN
    29:CCCCC       RLOD = SHUTDOWN LOOSENING FUNCTION, UGM/DM**2/MIN
    30:CCCCC       EXCHANGE RATE CONSTANTS ARE:
    31:CCCCC       A = MOBILE TO LOOSE DEPOSITION CONSTANT, 1/MIN
    32:CCCCC       B = LOOSE TO MOBILE RELEASE CONSTANT, 1/MIN
    33:CCCCC       CT = LOOSE TO TIGHT SINTERING CONSTANT, 1/MIN
    34:CCCCC       Y(1) IS LOOSE CRUD, Y(2) IS MOBILE CRUD
    35:CCCCC       YPRIME REPRESENTS TIME DERIVATIVE
    36:            REAL K,Y(N),YPRIME(N)
    37:            COMMON /PARAM/A,B,CT,RCS,PCMU,S,V,RLOU,RLOD,K
    38:            COMMON /VAR/QEM,EEMF,QLD,ISTOP
    39:            QEM = QLD+QEMF*EEMF
    40:            IF (ISTOP.EQ.1) THEN
    41:            RL = RLOD
    42:            ELSE
    43:            RL = RLOU*EXP(-K*X)
    44:            END IF
    45:            RPC = RCS+PCMU*QLD/V
    46:            YPRIME(1) = -(B+CT)*Y(1)+A/S*V*Y(2)+RL
    47:            YPRIME(2) = S/V*B*Y(1)-(A+QEM/V)*Y(2)+RPC
    48:            RETURN
    49:            END
EOF:49
```

INTERNAL DISTRIBUTION

1.	CW Anthony	105N	24.	CA Junghans	1100N	47.	H. Toffer	1118N
2.	DB Bechtold	1118N	25.	WEB Lander	1113N	48.	DJ Trimble	1118N
3.	JR Bolliger	1117N	26.	AP Larrick	1118N	49.	TV VanLear	105N
4.	JJ Bombino	FED	27.	JT Long	1105N	50.	RD Warner	1106N
5.	DF Brendel	1114N	28.	JJ McGuire	1117N	51.	RE Whiteside	105N
6.	PA Carlson	1114N	29.	JF McLaughlin	MW	52.	UNI Record	FED
7.	RA Cox	1101N	30.	RL Moffitt	1101N	53.	UNI File	FED
8.	DS Cunningham	1114N	31.	SR Morgan	FED	54.	Extra	FED
9.	TE Dabrowski	FED	32.	RW Ness	1101N	55.	Extra	FED
10.	HL Debban	1101N	33.	DJ Parmenter	105N	56.	Extra	FED
11.	JJ Dorian	1114N	34.	MA Payne	1101N	57.	Extra	FED
12.	BW Eakin	1101N	35.	GH Phillips	105N	58.	Extra	FED
13.	TE Edwards	1100N	36.	DR Pratt	1118N	59.	Extra	1118N
14.	BB Emory	1118N	37.	RJ Pyzel	1100N	60.	Extra	1118N
15.	GL Erickson	1703D	38.	DL Renberger	1117N	61.	Extra	1118N
16.	EL Etheridge	1101N	39.	RR Roehl	105N			
17.	DB Ferguson	105N	40.	WG Ruff	313			
18.	TA Galioto	1118N	41.	JP Schmidt	1101N			
19.	JM Garcia	1114N	42.	DW Simpson	1100N			
20.	LL Grumme	1113N	43.	GL Smith	1118N			
21.	SW Heaberlin	1118N	44.	RK Stafford	1101N			
22.	LL Humphreys	1117N	45.	JW Stiffler	1101N			
23.	GI Hutcherson	1115N	46.	DS Takasumi	1118N			

EXTERNAL DISTRIBUTION

62- 64. U. S. Department of Energy
Richland Operations Office
P. O. Box 490
Richland, Washington 99352

65-240. U. S. Department of Energy
Technical Information Center
Oak Ridge, Tennesee